

Green Chemistry

Accepted Manuscript



This is an *Accepted Manuscript*, which has been through the Royal Society of Chemistry peer review process and has been accepted for publication.

Accepted Manuscripts are published online shortly after acceptance, before technical editing, formatting and proof reading. Using this free service, authors can make their results available to the community, in citable form, before we publish the edited article. We will replace this *Accepted Manuscript* with the edited and formatted *Advance Article* as soon as it is available.

You can find more information about *Accepted Manuscripts* in the [Information for Authors](#).

Please note that technical editing may introduce minor changes to the text and/or graphics, which may alter content. The journal's standard [Terms & Conditions](#) and the [Ethical guidelines](#) still apply. In no event shall the Royal Society of Chemistry be held responsible for any errors or omissions in this *Accepted Manuscript* or any consequences arising from the use of any information it contains.



www.rsc.org/greenchem

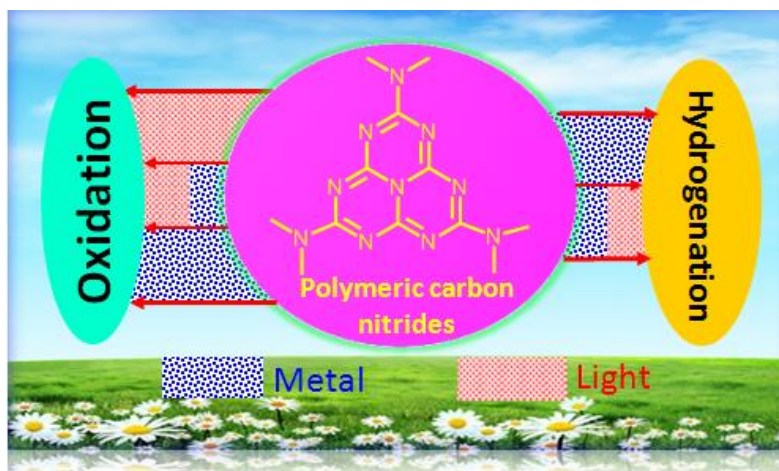
Graphitic carbon nitride polymers: Promising catalysts or catalyst supports for heterogeneous oxidation and hydrogenation

Yutong Gong, Mingming Li, Haoran Li, Yong Wang*

Carbon Nano Materials Group, ZJU-NHU United R&D Center, Center for Chemistry of High-Performance and Novel Materials, Key Lab of Applied Chemistry of Zhejiang Province, Department of Chemistry, Zhejiang University, 310028 Hangzhou, P. R. China.

Corresponding author. E-mail: chemwy@zju.edu.cn, Fax: +86-571-87951895

Graphical Abstract



The review summarizes recent oxidation and hydrogenation strategies catalyzed by g-C₃N₄ based systems.

Abstract:

Due to their industrial indispensability, the heterogeneous catalytic oxidation and hydrogenation continue to be hot topics in both experimental and theoretical studies. Graphitic carbon nitride (g-C₃N₄), thanks to its unique structure and thus excellent properties such as semiconductivity and nitrogen richness, is suitable to act as a metal-free catalyst or catalyst support for these two significant transformations. This critical review will summarize the recent significant advances achieved in the field of oxidation and hydrogenation realized by g-C₃N₄ based catalytic systems. The review covers the practical applications and brief mechanistic discussions in three broad catalytic cases, catalytic oxidation under light irradiation, catalytic oxidation without light illumination, and catalytic hydrogenation with g-C₃N₄ supporting metal nanoparticles. The state-of-the-art and future challenges of heterogeneous hydrogenation and oxidation by g-C₃N₄ based systems are also discussed.

1. Introduction

From an industrial point of view, heterogeneous catalysts not soluble in the same phase with the organic reactants have the inherent advantage of easy separation and very often also of better handling properties.¹ With the increasing demand for efficient organic transformations based on the concept of “Green Sustainable Chemistry”, the development of highly selective reaction systems using heterogeneous catalysts is greatly desired. Heterogeneous catalytic reactions are of great importance in almost all large-scale chemical conversion, energy production and pollution mitigation processes. It is found that over 90% of all commercial chemical processes involve the use of heterogeneous catalysts,² and not exaggeratively, heterogeneous catalysis plays a crucial role in the transformation of the chemical industry towards higher level of sustainability.

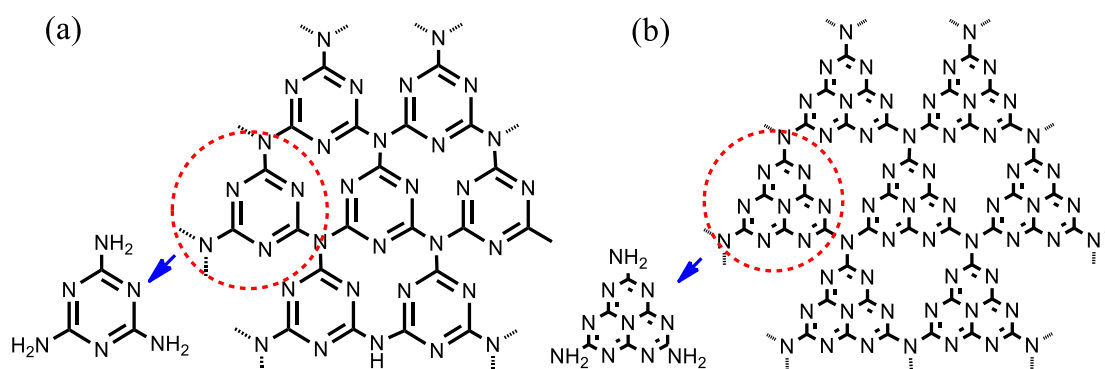
Selective oxidation and hydrogenation are two of the key synthetic steps for the activation of a broad range of substrates, and they are widely used for the production of either finished products or intermediates.³ Oxidation is an important method to bring functionality into petroleum-based feedstocks, and it is often the first step to high-value fine chemicals, agrochemicals, and pharmaceuticals.⁴ Hydrogenation is a common process to reduce or saturate organic compounds such as vegetable oils.⁵⁻⁸ However, the traditional oxidation processes employing stoichiometric inorganic oxidants are under increasing environment pressure,⁹⁻¹⁰ and available non-catalytic hydrogenations always take place only at very high temperatures or pressures. Therefore, the seeking for highly efficient catalytic oxidation and hydrogenation systems remains a continuous hot topic in industrial manufacture, and the development of suitable heterogeneous catalysts has always been the focus of the endeavors.

Actually, scientists have spent tremendous efforts on the development of effective heterogeneous catalysts for oxidation and hydrogenation. Early successful example of liquid phase oxidation catalyst is the Ti(IV)/SiO₂ which was commercialized by Shell in the 1970s for the production of propene oxide. The development of titanium silicalite (TS-1) by Enichem scientists in the mid-eighties

was another benchmark.¹¹ Over the past 30 years, heterogeneous catalysts for oxidation have covered various metal-free systems, metal oxides,¹² molecular sieves,¹³ supported noble metal nanoparticles,^{1, 14-16} metal organic frameworks (MOF),¹⁷ *etc.* The heterogeneous catalysts for hydrogenation are also either in the form of bio-, heterogeneous and heterogenised homogeneous catalysts. These heterogeneous catalysts have touched the hydrogenations of alkenes, alkynes, aromatics, aldehydes, ketones, esters, carboxylic acids, nitro groups, nitriles and imines, *etc.* Among the catalysts investigated, the most effective heterogeneous catalysts for oxidation and hydrogenation reactions usually contain a metal supported on a carrier, notably, both of which significantly alter catalytic performance. For example, among the various metals employed in the hydrogenation process, Ni, Pd and Pt in group 10 are the ones intensively studied and they show diverse catalytic performance. Besides varying metals, the selection of supports is a pivotal factor deciding the catalytic effect. For example, compared with traditional supports such as SWNT-SiO₂, activated carbon, TiO₂, and Al₂O₃ *etc.*, nitrogen-doped carbon showed unprecedented facilitating effect for Pd nanoparticles to catalyze the hydrogenation of vanillin.¹⁸ In the case of benzyl alcohol oxidation, various support materials such as oxides (*e.g.*, MgO,¹⁹ CeO₂,²⁰ TiO₂,²¹ SiO₂²²), zeolites,²³ MOFs,²⁴ carbon in different forms²⁵⁻²⁷ are applied to support Pd or Au nanoparticles. They showed diverse activities and selectivities due to the different interaction between the noble metal particle and supports. The surface chemistry and morphology of the support would influence the oxidative states and electronic properties of the metal nanoparticle and thus the catalytic performance. Lately, graphitic carbon nitride (g-C₃N₄) has drawn considerable attention in catalysis as it shows interesting photochemical properties and the chemical and physical features which make it an ideal choice for both metal-free catalyst and positive catalyst support.

The study of carbon nitride (C₃N₄) started from 1830s when Berzelius and Liebig made a polymeric derivative and named it as “melon”.²⁸ It was followed by many theoretical studies²⁹⁻³⁴ until g-C₃N₄ was demonstrated to be the most stable allotrope of carbon nitride under ambient conditions.^{33, 35-37} Since then, more research has

focused on the study of $g\text{-C}_3\text{N}_4$ materials with expectations for further understanding of carbon nitrides.³³ Owing to lack of experimental data, there is a prevailing discussion about the actual existence of a graphitic material with idealized composition C_3N_4 and possible structure models for $g\text{-C}_3\text{N}_4$. Inspired by the structure of graphite, triazine (C_3N_3) had been put forward as the elementary building block of $g\text{-C}_3\text{N}_4$ (Scheme 1a).^{33, 35-54} However, another possible building block, tri-s-triazine (heptazine) rings, which are structurally related to the hypothetical polymer melon,^{28-29, 55-58} have recently shown to be energetically favored with respect to the triazine-based modification (Scheme 1b).^{51, 59} The tri-s-triazine rings are cross-linked by trigonal nitrogen atoms, and very recent work has shown that indeed the pyrolysis of cyanamide, dicyandiamide, or melamine yields a melon polymer built up from melem units,^{42, 51, 59-66} confirming that this tecton is the most stable local connection pattern. Ideally condensed $g\text{-C}_3\text{N}_4$ consists of only carbon and nitrogen atoms with a C/N molar ratio of 0.75. However, up to now, no perfectly condensed $g\text{-C}_3\text{N}_4$ was fabricated and the existing $g\text{-C}_3\text{N}_4$ architectures are rich in defects and they are as-grown polymer materials which are not single crystals. Therefore, $g\text{-C}_3\text{N}_4$ can be seen as a family of layered graphitic carbon nitride compounds with C/N ratio close to 0.75.



Scheme 1. s-Triazine (a) and tri-s-triazine (b) as tectons of $g\text{-C}_3\text{N}_4$.

Besides the similar microstructure of graphite and $g\text{-C}_3\text{N}_4$, their physicochemical properties greatly differ. In appearance, $g\text{-C}_3\text{N}_4$ is yellow while graphite is black. When it comes to the electronic properties, the two materials are thoroughly different.⁶⁷ The graphite reveals excellent conductivity in the dimensions of the layers while $g\text{-C}_3\text{N}_4$ is characterized to be a wide-band semiconductor.⁶⁸ Therefore, $g\text{-C}_3\text{N}_4$

is a promising alternative candidate for photosensitive catalyst. Defective features in accessible g-C₃N₄ are not favorable for theoretical studies about the structure. Nevertheless, surface terminations and defects seem to be the real active sites in heterogeneous catalysis. These defects provide access for chemical modifications, which is preferable in catalyst property manipulation.⁵⁴ Beyond that, the prepared g-C₃N₄ possesses many other fascinating characteristics which make it suitable as a metal-free catalyst or a desired catalyst support. Notably, the nitrogen richness, incompletely condensed amino functions together with tertiary and aromatic amines in the architecture make it a Lewis basic catalyst, supplying abundant active sites for metal-free catalysis.⁶⁹ Further, the rich nitrogen content also supplies abundant anchoring sites for metallic nanoparticles when g-C₃N₄ used as heterogeneous catalyst support.⁷⁰ More importantly, as an organic polymer semiconductor that can develop delocalized electron states, the metal particles and g-C₃N₄ are not independent. The work functions of most noble metals are located between the conduction band and valence band of g-C₃N₄. Metal particles with higher work function can give an elevated Schottky barrier, and thus enhanced charge separation at the interface of the metal-semiconductor heterojunction.⁷¹ The enhanced charge separation has great impact on the catalytic performance of the catalyst. Therefore, g-C₃N₄ would do more than a just a metal carrier, but also an “active support” that promotes the catalytic activity or selectivity of the metal particles.

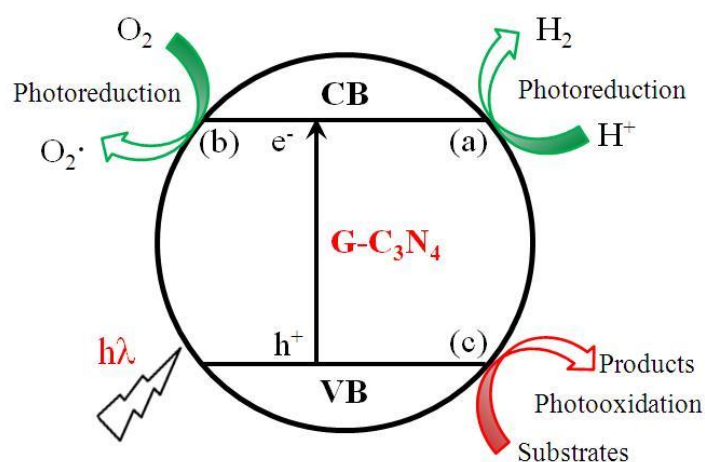
Based on these properties, the applications of g-C₃N₄ have been extended to material science, catalysis, electronic and optical fields. To date, some inspiring reviews about the preparation, properties and wide applications were given by many groups since the use as metal-free Friedel-Crafts catalyst reported by Antonietti *et al.*⁷²⁻⁷³ The introduction of g-C₃N₄ as catalyst or catalyst support for oxidation and hydrogenation, at least based on current works, is a nice way for developing efficient and sustainable catalysts, while this is indeed a young topic, yet full of promise. Until now, the significant progress in this area has not been specifically reviewed yet. Therefore, a summary of this topic will be very meaningful and interesting to the wide readerships of *Green Chem.* We would like, therefore, to afford a review regarding

the catalytic oxidations and hydrogenations based on carbon nitrides, especially those selective oxidation and hydrogenation reactions in liquid phase, and highlight the catalytic mechanism together with catalyst design strategy, hoping that much more breakthroughs will be achieved in this direction and boost the heterogeneous catalysis towards sustainable chemistry.

2. Catalytic oxidation by g-C₃N₄ based systems

2.1 Oxidations under visible light illumination

As mentioned, g-C₃N₄ is a polymeric semiconductor whose HOMO derives from pz orbitals of nitrogen atoms and LUMO predominantly consists of pz orbitals of carbon atoms. The band gap is calculated to be 2.6 eV, with the edges of the conduction band and valence band lying at -1.0 V and +1.6 V (vs. NHE).⁶⁸ Thus, the properties allow it to be photosensitive, where the photo-induced electron can reduce O₂ to active •O₂⁻ (Scheme 2b). Therefore, it can be envisioned that g-C₃N₄ would act as a desirable visible light responsive photocatalyst for the oxidation of alkanes, olefins, and alcohols, *etc.*



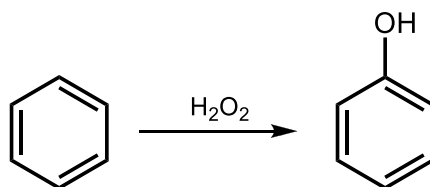
Scheme 2. Visible light induced photocatalysis by g-C₃N₄: (a) hydrogen evolution from water, (b) photochemical activation of O₂, and (c) photocatalytic oxidation or degradation of organic substrates.

2.1.1 By metal-free g-C₃N₄ or doped g-C₃N₄

The conversion of alkanes into oxygen-containing compounds is one of the most important and fundamental transformations in industrial chemistry.⁷⁴ Higher alkanes and alkyl aromatic hydrocarbons can be oxidized by heating them under oxygen at

rather high temperatures through a radical-chain autooxidation.⁷⁵ However, the autooxidation is characterized by poor selectivity. Furthermore, industrially performed catalytic oxidation reactions often suffer from other drawbacks such as lack of catalyst recycling and negative environmental impact because of the use of toxic metal catalysts.⁷⁵⁻⁷⁶ As a consequence, the exploration of effective metal-free catalysts has never stopped. Photo-responsive catalysts such as g-C₃N₄ provide sufficient potential solutions.

Phenol is an important commodity chemical.⁷⁷⁻⁷⁸ In industry, phenol has been mainly produced from benzene by the three-step cumene process, which generates large amounts of waste.⁷⁹ An ideal process should be the direct oxidation of benzene to phenol with clean oxidants, such as molecular oxygen or hydrogen peroxide (Scheme 3).⁸⁰ In this regard, it was recently found that carbon nitride is indeed an active metal-free photocatalyst with high selectivity for direct oxidation of benzene to phenol under mild conditions.⁸¹



Scheme 3. Direct oxidation of benzene to phenol.

Using hydrogen peroxide as a clean oxidant, at a reaction temperature of 60 °C and under the irradiation of visible light ($\lambda > 420$ nm), fluorine-doped carbon nitrides (CNF) showed improved activities compared to bare g-C₃N₄ in the catalytic oxidation of benzene to phenol. The result showed that with g-C₃N₄ as a catalyst, phenol was formed with a very low turnover frequency (TOF) of 0.006 h⁻¹, which can be enhanced to a TOF of 0.125 h⁻¹ using CNF-2.0.⁸²

Selective oxidation of primary alcohols to aldehydes is another highly relevant transformation in organic chemistry due to the properties and chemical reactivity of these carbonylic compounds.^{21, 83-85} Su and coworkers found that mesoporous g-C₃N₄ (mpg-C₃N₄) was effective to activate molecular oxygen for the oxidation of benzyl alcohol to benzaldehyde with more than 99% selectivity and 57% conversion under

visible light irradiation for 3 h at 100 °C.⁸⁶ Both electron-withdrawing and electron-donating substituents enhanced the rate of the reaction. Mechanism investigations by electron spin resonance (ESR) demonstrated that the photoelectron assisted the generation of $\bullet\text{O}_2^-$ radicals which helped deprotonate the alcohol. Then the alkoxide anion would react with the positive hole and the superoxide radical to form corresponding aldehyde/ketone. Besides introducing mesoporosity, acid treatment of g- C_3N_4 also promoted the transformation of benzyl alcohol to benzaldehyde.⁸⁷ Among all acids tested, sulfuric acid-modified g- C_3N_4 showed the highest catalytic activity and gave benzaldehyde with 23% yield over 4 h under visible light irradiation, which was about 2.5 times higher than that of pristine g- C_3N_4 . The improved surface area, reduced structural size, enlarged band gap, enhanced surface chemical state, and facilitated photoinduced charge separation after acid modification were responsible for the enhanced photocatalytic activity. Wang *et al.* revealed that the oxidation of aromatic over mpg- C_3N_4 could proceed smoothly in aqueous phase under visible light. More importantly, the mpg- C_3N_4 exhibited strong resistance to strongly acidic conditions and demonstrated no deactivation after cycling.⁸⁸

Very recently, thiophene motif decorated mpg- C_3N_4 materials were fabricated via copolymerization of 3-aminothiophene-2-carbonitrile (ATCN) and dicyanamide (MCN-ATCN_x, x refers to weighted-in amount of ATCN).⁸⁹ The band gap of the obtained semiconductors decreased with the increase of the ATCN and the best performance for oxidation of benzyl alcohol to benzaldehyde was obtained by MCN-ATCN_{0.05} with 53% conversion and >99% selectivity under visible light (Table 1). MCN-ATCN_{0.05} was also effective in catalyzing other various p-substituted benzyl alcohols and it was found that the reaction rate was enhanced by electron-donating substituents while retarded by electron-withdrawing ones. According to the ESR studies, the authors declared that the primary alcohol oxidation was a combined action of $\bullet\text{O}_2^-$ and singlet oxygen ($^1\text{O}_2^-$) instead of a process intermediated by only $\bullet\text{O}_2^-$.⁸⁹

Table 1. Physicochemical properties and photocatalytic activity of bulk g-CN, MCN and MCN-ATCN_x samples for selective oxidation of benzyl alcohol driven by light irradiation,^a adapted from Ref. ⁸⁹.

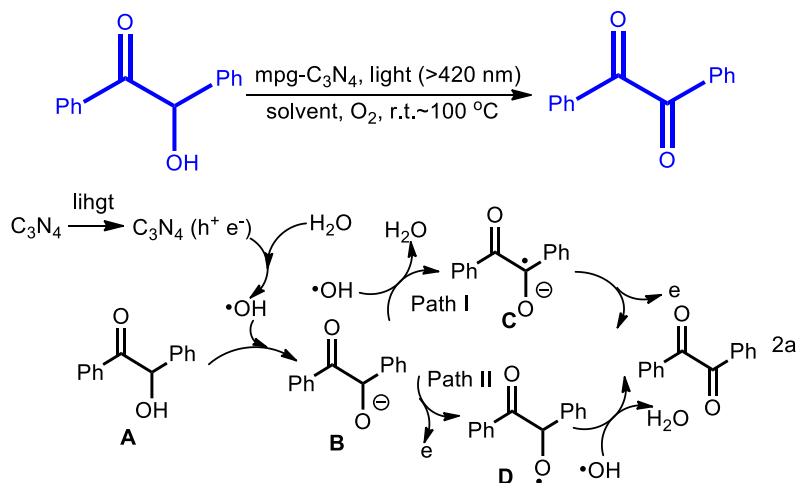
c1ccc(cc1)CO
 $\xrightarrow[\text{Wavelength } >420 \text{ nm}]{60 \text{ }^\circ\text{C}, 3 \text{ h}, 1 \text{ bar O}_2}$
c1ccc(cc1)C=O

Entry	Sample	S _{BET} (m ² g ⁻¹)	Band gap (eV)	hν	Conv. [%]	Sel. [%]
1	Blank	/	/	+	<1	/
2	CN	9	2.76	+	<1	/
3	MCN	230	2.75	+	19	>99
4	MCN-ATCN _{0.01}	223	2.68	+	32	>99
5 ^b	MCN-ATCN _{0.05}	227	1.88	+	53	>99
6	MCN-ATCN _{0.05}			-	<1	/
7	MCN-ATCN _{0.05}			+	13	>99
8	MCN-ATCN _{0.05}			-	<1	/
9	MCN-ATCN _{0.1}	219	1.85	+	28	>99

^a Reaction conditions: 5 mg Cat., 0.1 mmol benzyl alcohol, 1.5 ml trifluorotoluene, O₂ (1 bar), 60 °C, 3 h, λ > 420 nm. ^b Reaction under 100 °C for 5 h with λ > 600 nm cut-off filter.

Mpg-C₃N₄ has also been proved to be active for the oxidation of α-hydroxy ketones to 1,2-diketones, an important synthetic building block for the construction of complex structures in organic chemistry, by Zheng *et al.*⁹⁰ 72% yield of the target product was achieved at 100 °C under 1 atm O₂ for 10 hours in acetonitrile which was characterized to be the optimal reaction condition. Electron-withdrawing and -donating substituents as well as *ortho*-substitution on the aryl ring were all well tolerated. A plausible mechanism of photocatalysis reaction was also described. Firstly, the holes were combined with the hydroxyl to generate the hydroxy radical anion (•OH), which was formed by the irradiation of mpg-C₃N₄. The deprotonation of 2-hydroxy-1, 2-diphenylethanone occurred in the presence of •OH to form intermediate B which had two possible ways to generate the product. Path I:

intermediate B by deprotonation was to form intermediate C, which lost an electron to produce the 2a, while path II lost an electron to form D, which was deprotonated to give product 2a (Scheme 4).

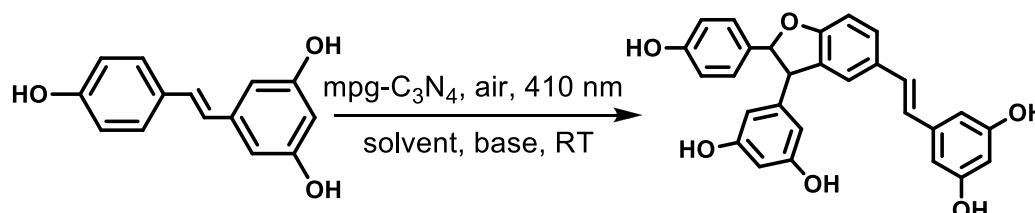


Scheme 4. A possible reaction mechanism for the oxidation of α -hydroxy ketones to 1,2-diketones, adapted from Ref.⁹⁰.

N-H oxidation allows the generation of a number of active nitrogen-containing compounds as intermediates of various chemically and biologically significant molecules.⁹¹⁻⁹² Under the illumination of visible light, mpg-C₃N₄ can promote the oxidation of amines into imines, which then undergo consecutive reactions. Under optimized conditions, complete conversion of benzylamine into N-benzylidene benzylamine was obtained in 3.5 h. Note that this protocol could be successfully extended to other substrates, such as benzylamines substituted with electron-donating and electron-withdrawing groups, and heterocyclic amines containing nitrogen and sulfur atoms which usually poison most metal catalysts. Specifically, a simple and efficient synthesis of benzoxazoles, benzimidazoles, and benzothiazoles could be realized through a one-pot synthesis by this photocatalytic cascade reaction with high yields.⁹³ The authors also advanced this catalytic system to the oxidative coupling of N-phenyl-1,2,3,4-tetrahydroisoquinoline derivatives with nitromethane or other nucleophiles with good to excellent yields under visible light.⁹⁴

Mpg-C₃N₄ was successfully employed as a desired photocatalyst in the aerobic oxidative coupling of resveratrol and its analogues by Liu and coworkers recently.⁹⁵ Resveratrol and its analogues, as a class of vital compounds in drug development,

were frequently explored as potential building blocks for the construction of more complicated oligomers such as δ -viniferin and its analogues with excellent bioactivity.⁹⁶⁻⁹⁸ As for the lack of reports on the production of δ -viniferin by the aerobic oxidative coupling of resveratrol at room temperature, the authors proved that mpg-C₃N₄ was a highly suitable photocatalyst for the reaction (Scheme 5).



Scheme 5. Oxidative coupling of resveratrol to δ -viniferin, adapted from Ref.⁹⁵.

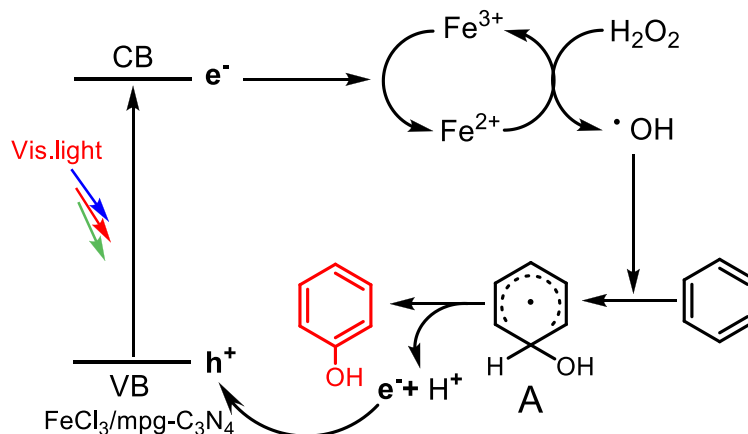
The best result (86% yield, 79% conversion) was obtained when the reaction was performed with 2,6-lutidine as a desired base and acetonitrile as the superior solvent under bubbled air and visible light illumination. Control experiments also showed that the presence of photocatalyst, oxidant, and light source is necessary for the desired reaction to proceed. After the optimization of the reaction conditions, a series of resveratrol analogues were subjected to this reaction system. Results showed that methoxylated and acetylated analogues of resveratrol, electron-neutral, -donating and withdrawing substitutes as well as sterically modified substrates all demonstrated moderate to high yields. A proposed mechanism indicated that the $\bullet\text{O}_2^-$ generated by the electron-transfer pathway between mpg-C₃N₄ and molecular oxygen was the vital reactive oxygen species (ROS) in the initial step of the radical coupling pathway.

2.1.2 G-C₃N₄ coupled with other redox catalysts

Metal/g-C₃N₄ system

As described above, satisfactory selectivity was obtained by g-C₃N₄ and doped g-C₃N₄ for the oxidation of benzene to phenol. Better conversion is another goal to chase. Combination of g-C₃N₄ with metals could offer another optional choice to raise the photocatalytic activity.^{81, 99} Under the same reaction condition, a TOF of 14.8 h⁻¹ was achieved by using Fe-g-C₃N₄/SBA-15 as a photocatalyst,⁸¹ which was much better than the pure g-C₃N₄ system (TOF=0.006 h⁻¹).⁸² Our group recently presented the preparation of FeCl₃/mpg-C₃N₄ hybrids and their largely enhanced photocatalytic

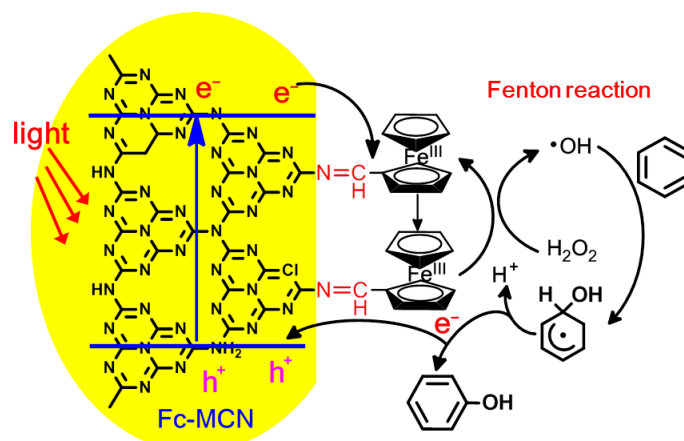
activity in the oxidation of benzene to phenol, which could favorably activate H_2O_2 for the oxidation with 23% conversion ($\text{TOF}=17 \text{ h}^{-1}$).¹⁰⁰ The result revealed the synergistic effect of Fe species and mpg- C_3N_4 . ESR measurement reflected that mpg- C_3N_4 could promote the reduction of Fe^{3+} to Fe^{2+} during the catalytic process, thus facilitated the decomposition of H_2O_2 to $\cdot\text{OH}$ radical which accelerated the overall reaction (Scheme 6).



Scheme 6. A possible reaction mechanism for the catalytic oxidation of benzene by $\text{FeCl}_3/\text{mpg-C}_3\text{N}_4$ hybrids,¹⁰⁰ reproduced by permission of The Royal Society of Chemistry.

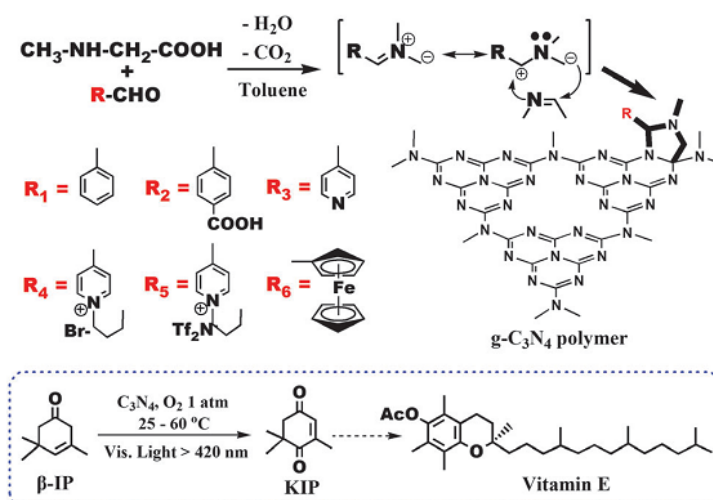
$\text{Fe-C}_3\text{N}_4$ was deposited into the titanium silicate zeolite (TS-1) and applied for the oxidation of benzene to phenol as well.¹⁰¹ The catalytic activity improved obviously under visible light irradiation in a biphasic water- H_2O_2 /acetonitrile medium. However, the catalyst showed inferior stability owing to the lack of strong chemical interaction between $\text{Fe-C}_3\text{N}_4$ and TS-1 host.

Ferrocene moieties (Fc) were recently heterogenized onto mpg- C_3N_4 by covalent -C=N- or -N-CO- linkages.¹⁰²⁻¹⁰³ The band-gap structure of Fc-mpg- C_3N_4 shifted to lower energies compared to mpg- C_3N_4 which was attributed to the enlargement of p-conjugated electron delocalization at the surface of the material improving the absorption cross-section for the incident light. The photocatalytic activities of the Fc-mpg- C_3N_4 for the oxidation of benzene to phenol increased with the increasing Fc content. The synergistic donor-acceptor interaction between the carbon nitride matrix and Fc group, improved exciton splitting, and coupled photocatalytic performance allowed the direct synthesis of phenol from benzene (Scheme 7).



Scheme 7. Merging of the redox function of ferrocene with carbon nitride photocatalysis to construct a heterogeneous photo-Fenton system for direction hydroxylation of benzene to phenol, adapted from Ref.¹⁰².

Our group recently developed the organic groups decorated mpg-C₃N₄ prepared via 1,3-dipolar cycloaddition of azomethine ylides (Prato's reaction), in situ generated by thermal condensation of thea-amino acid N-methylglycine and an aldehyde containing R group (Scheme 8).¹⁰⁴ The absorbance of the carbon nitride materials with the linked organic groups was significantly red shifted in comparison with the mpg-C₃N₄. The C₃N₄-R6 containing ferrocene favorably moved the absorption edge to >700 nm, covering most of the sunlight spectrum. Moreover, the optical band gaps of modified samples were narrowed, for instance: C₃N₄-R4 showed a band gap of 2.20 eV.

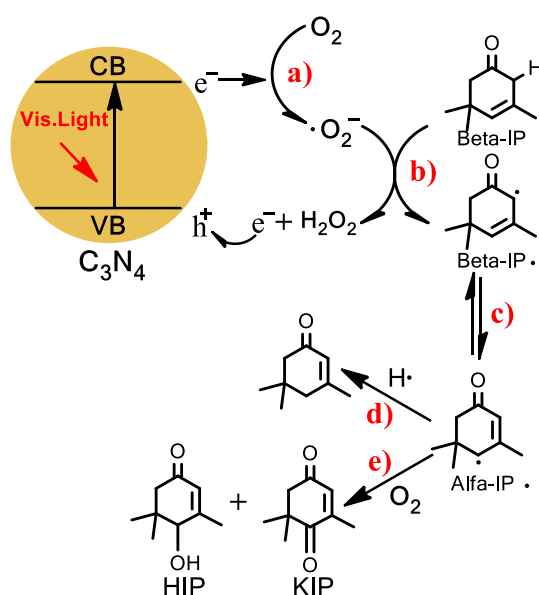


Scheme 8. The 1,3-dipolar cycloaddition reaction for carbon nitride modification, and the industrial route for vitamin E production via selective oxidation of

beta-isophorone to keto-isophorone,¹⁰⁴ reproduced by permission of The Royal Society of Chemistry.

The narrowed band gap and extended visible light absorption range of the modified mpg-C₃N₄ motivated us to apply them for the photocatalytic aerobic oxidation of beta-isophorone (β -IP) to keto-isophorone (KIP) which is a widely-used chemical and is an intermediate in preparing foodstuffs, vitamins and carotenoids. It showed that C₃N₄-R4 and C₃N₄-R6 afforded higher β -IP conversion and KIP selectivity than the parent mpg-C₃N₄. Satisfactory KIP yield (Conv.: 96%; Sel.: 82%) was reached over C₃N₄-R6 at 60 °C.¹⁰⁴

The photo-induced electrons from the conduction band of mpg-C₃N₄ is capable of reducing O₂ to $\bullet\text{O}_2^-$ (Scheme 2, Scheme 9a).^{86, 93, 105-106} It is reasonable to assume that the H-abstraction in β -IP by the $\bullet\text{O}_2^-$ radical can occur, because the C-H bond at the 2 site of β -IP holds a relatively low bond dissociation enthalpy (75.78 kcal mol⁻¹) and the resulting β -IP \bullet radicals are significantly stabilized by allylic resonance (Scheme 9b and c).¹⁰⁷ Following a radical route, the O₂ kinetic addition could then occur on the α -IP \bullet radical, the one with favorable dioxygen-binding affinity, and finally form the main products (KIP and HIP) via the decomposition of α -IP peroxide (Scheme 9e).¹⁰⁷ Therefore, the generation of superoxide radical anion $\bullet\text{O}_2^-$ is a vital step for the whole oxidation. In comparison to mpg-C₃N₄, an enhanced Lorentzian line (Centering at g= 2.0031) from C₃N₄-R6 was observed in ESR spectra, revealing more unpaired electrons on conjugated C₃N₄-R6 aromatic rings, which would contribute to more $\bullet\text{O}_2^-$ anions, and this should be considered as the origin of higher catalytic activity of C₃N₄-R6.



Scheme 9. Proposed mechanism for the oxidation of β -IP by carbon nitride polymers,¹⁰⁴ reproduced by permission of The Royal Society of Chemistry.

C_3N_4 /Au nanocomposite was demonstrated effective for the transformation from cyclohexane to cyclohexanone with conversion efficiency of 10.54% and 100% selectivity.¹⁰⁸ Under visible light, H_2O was oxidized to H_2O_2 by C_3N_4 and then decomposed into hydroxyl radicals ($HO\cdot$), which served as a strong oxidant for conversion of cyclohexane to cyclohexanone. In the process, Au nanoparticles under visible light played a key role in the eventual high conversion and selectivity under Xe lamp irradiation without initiator or oxidant (Scheme 10).

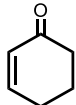
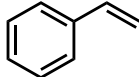
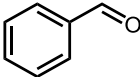
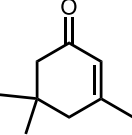
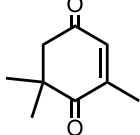
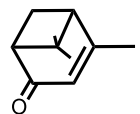


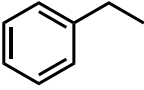
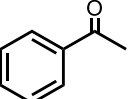
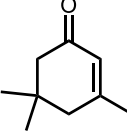
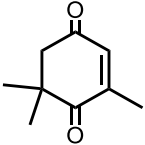
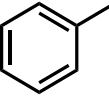
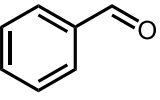
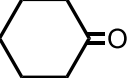
Scheme 10. Proposed reaction mechanism for visible-light driven oxidation of cyclohexane on C_3N_4 /Au,¹⁰⁸ reproduced by permission of The Royal Society of Chemistry.

G-C₃N₄/organocatalyst system

Some organocatalysts such as 1-hydroxybenzotriazole (HBT), N-hydroxysuccinimide (NHSI) and N-hydroxyphthalimide (NHPI) can activate O₂ during the oxidation reaction. However, co-catalyst is always necessary for the N-hydroxy (>N-OH) compounds to generate the active N-oxyl radical (>N-O•).¹⁰⁹⁻¹¹¹ As has been proven that g-C₃N₄ can activate O₂ to •O₂⁻ under the illumination of visible light,^{86, 93, 112-114} if •O₂⁻ can abstract a hydrogen from >N-OH, the formed >N-O• radical could smoothly activate the C-H bond. Our group applied g-C₃N₄/NHPI system for the selective allylic oxidation of cholesteryl acetate (CA) to 7-ketocholesteryl acetate (7-KOCA), which is a key step in the synthesis of vitamin D₃.¹¹⁵⁻¹¹⁸ In this metal-free catalytic system, 48% conversion and >99% selectivity for 7-KOCA were attained at 35 °C within 8 h, and various extended substrates were also proceeded with satisfying activities and selectivities (Table 2).¹⁰⁶ The same combination of g-C₃N₄/NHPI was reported by Wang *et al.* for the oxidation of α-isophorone into ketoisophorone at evaluated temperature (130 °C) in the absence of light.¹¹⁹

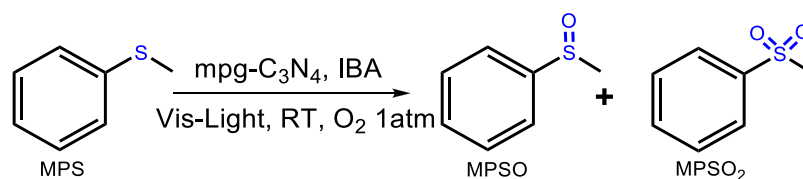
Table 2. The results of the oxidation of various substrates with g-C₃N₄ and NHPI,^a adapted from Ref.¹⁰⁶.

Entry	Substrate	Product	Time [h]	Conv. [%]	Sel. [%]
1			8	93	77
2 ^b			8	92	71
3 ^c			8	90	66
4 ^d			8	95	67
5			24	33	70
6			20	26	79
7 ^e			18	71	66

8			23	27	84
9 ^f			4.5	100	>99
10			20	9	>99
11 ^g			24	6	>99

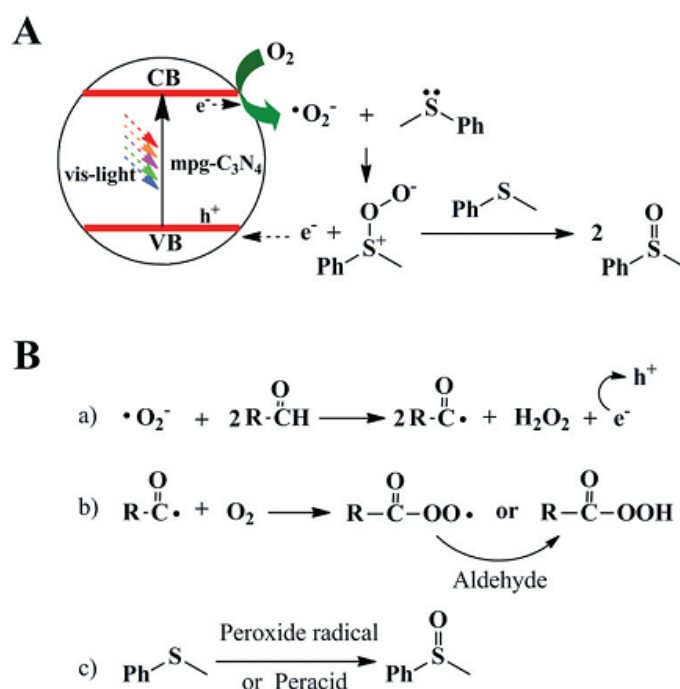
^a Reaction conditions: substrates (10 mmol), g-C₃N₄(100 mg), NHPI (1 mmol), acetonitrile (20 mL), O₂ 1 atm, 60 °C, under visible light irradiation. ^b Second run to test the reusability of catalyst. ^c Third run to test the reusability of the catalyst. [d] Fourth run to test the reusability of the catalyst. ^e Benzonitrile (20 mL) as solvent. ^f g-C₃N₄ (50 mg) and NHPI (0.5 mmol) were used. ^g g-C₃N₄ (50 mg) and NHPI (0.1 mmol) were used.

Aldehydes are another kind of organic radical initiators. They will undergo autoxidation in the presence of O₂. Interestingly, when a mixture of an aldehyde and another organic substrate is submitted to molecular oxygen, the autoxidation of the aldehyde will promote the oxidation of the less reactive partner.¹²⁰ The oxidation of sulfides to sulfoxides can be achieved with excessive amount of aldehyde (~5 equiv).¹²¹ We found that mpg-C₃N₄ could accelerate the autoxidation rate of isobutyraldehyde (IBA), which contributed to the formation of the corresponding acyl radical.¹⁰⁵ Both IBA and mpg-C₃N₄ alone showed minor activities for the oxidation of MPS. Without IBA, MPS conversion of 8% and selectivity of 99 % for MPSO was observed over mpg-C₃N₄ after 8 h while IBA afforded a conversion of 3% and selectivity of 97% without mpg-C₃N₄. A highly improved conversion of 97% and selectivity up to 98% for MPSO was gained in 4 h by the cooperation of mpg-C₃N₄ and IBA (Scheme 11).



Scheme 11. Oxidation of MPS by mpg-C₃N₄ and IBA, adapted from Ref.¹⁰⁵.

The possible reaction pathways with and without IBA were discussed. The $\bullet\text{O}_2^-$ was formed by the photogenerated electron-induced reduction of O_2 during light irradiation, which was confirmed by the ESR signal. It could attack the sulfur atom with the assistance of the positively charged hole (h^+), leading to the formation of the reactive intermediate persulfoxide or thiadioxirane in the absence of IBA. The electrophilic intermediate would react with starting material to afford two molecules of the sulfoxide product (Scheme 12a). Then the synergistic effect of mpg- C_3N_4 and IBA was studied by control experiments and ESR results. The concluded reaction mechanism was proposed as Scheme 12b. Firstly, the active $\bullet\text{O}_2^-$ radical oxidizes two molecules of aldehydes to the corresponding acyl radicals by injecting an electron into the valence band of mpg- C_3N_4 . Then, reacting with O_2 , the acyl radical forms a peroxide radical or peracid as intermediates containing active oxygen, which can smoothly oxidize sulfides to the corresponding sulfoxides.¹²²



Scheme 12. A possible reaction mechanism for the catalytic cycle of the mpg- C_3N_4 and mpg- C_3N_4 -aldehyde system,¹⁰⁵ reproduced by permission of The Royal Society of Chemistry.

2.2 Oxidations in dark

G-C₃N₄ bears multiply structural defects. The nitrogen functionalities on the surface might act as strong Lewis base. It holds full potentials as a heterogeneous metal-free catalyst in the absence of light irradiation. Studies upon sustainable oxidation demonstrated that g-C₃N₄ or modified g-C₃N₄ could be indeed directly employed as effective catalysts for the oxidation of cyclic olefins, alcohols, toluene and benzene.¹²³⁻¹²⁶

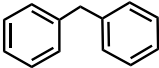
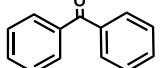
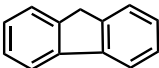
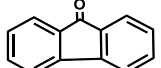
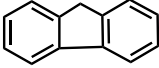
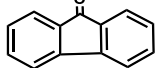
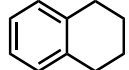
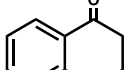
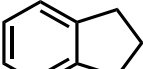
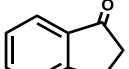
2.2.1 By g-C₃N₄, heteroatom-doped g-C₃N₄ and g-C₃N₄ based composites

Selective oxidation of primary carbon hydrogen bonds is of great importance in organic synthesis.¹²⁷ Green, efficient, and selective oxidation techniques are highly sought after in the chemical and pharmaceutical industry.¹²⁷⁻¹³⁰ Toluene is a typical alkyl aromatic molecule and the starting point for the production of aromatic alcohols, aldehydes or esters. When oxygen is employed as the terminal oxidant, the oxidation of toluene could proceed with high selectivity towards benzaldehyde at relatively low conversions.¹²⁵ Although giving high selectivities, bare g-C₃N₄ and mpg-C₃N₄ exhibited very low catalytic activity. Recently known materials modification strategies like heteroatom doping such as doping of boron atom in the matrix of carbon nitride has proven to significantly promote the catalytic oxidation activity of carbon nitride. For instance, g-C₃N₄ itself gave minor conversion of 2% in the oxidation of toluene, whereas boron-doped carbon nitride (CNB_{0.15}) provided a conversion up to 6.3% at 100% selectivity toward benzaldehyde.¹²³ The improvement was also observed in the case of ethylbenzene oxidation. This high selectivity toward benzaldehyde or acetophenone is very critical to industrial applications. In industry, the conversion of toluene has to be kept at less than 4% to attain 70% selectivity of benzaldehyde and to avoid the formation of carboxylic acid; however, heavy-metal catalysts as well as high temperature above 200 °C are used.¹³¹⁻¹³² Thus, it seems that a boron-doped carbon nitride could be a feasible solution. The main challenges are the maintenance of high selectivity at a conversion above 8% and the avoidance of catalyst deactivation.

When oxygen was taken as the oxidant, bare g-C₃N₄ is insufficient in promoting oxidation of inert hydrocarbons which is presumably due to its rather mild oxidation

potential as determined by its HOMO position.¹²³ Nevertheless, oxidation of hydrocarbons with an activated benzylic position went smoothly, even with O₂ as the oxidant. Again, the boron-doped carbon nitrides show improved catalytic activity, but even bare carbon nitride gave good conversions and high selectivity using molecular oxygen as clean oxidant (Table 3).

Table 3. Oxidation with molecular oxygen of substituted aromatics to ketones using CNB_{0.15} as metal-free catalyst,^a adapted from Ref.¹²³.

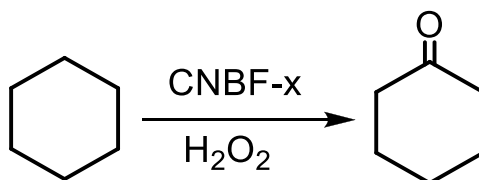
Entry	Substrate	Main Product	BDE ^b	T [°C]	Conv. [%]	Sel. [%]
1			81	160	20.3	95.1
2			80	130	45.7	>99.0
3 ^c			80	130	28.8	>99.0
4			83	130	72.2	87.5
5			82	115	36.7	>99.0

^a Reaction conditions: 1 mmol substrates, O₂ pressure 1 MPa, 50 mg catalyst, 4 mL acetonitrile, reaction time 24 h. ^b α_{C-H} bond dissociation energy from the literature. ^c Using g-C₃N₄ as a catalyst.

Park *et al.* found that mesoporous carbon nitrides synthesized by urea/formaldehyde (UF-MCN) can promote the oxidation of cyclic olefins with different ring sizes (cyclopentene, cyclohexene and cyclooctene).¹³³ The best catalytic performance was observed in the case of cyclooctene with 80.6% conversion and 92% selectivity for epoxide, while in the case of cyclopentene and cyclohexene, lower conversion and low selectivity for epoxide were observed. The reasons for conversion differences may correlate to the conformation, the bond angle strain and the torsional strains of cyclic olefins.¹³⁴ The catalytic activity was attributed to the oxygen functionalities which could facilitate the oxidation at mild conditions using H₂O₂ as

an oxidant. Reports of the same group declared that the presence of CO₂ showed a promotional effect for both the oxidation of cyclic olefins and aromatic alcohols when using carbon nitrides as the catalyst.^{124, 135}

The selective oxidation of cyclohexane to cyclohexanone is a very important industrial process, such as in the production of adipic acid and caprolactam, which in turn are the starting materials for the synthesis of nylon-6 and nylon-66 polymers, respectively.¹³⁶⁻¹³⁸ The homogeneous metal catalysts involved industrial process not only suffers from low conversion but also produces several products, such as mono- and dicarboxylic acids, esters, and other oxygenated materials which lead to tedious separation steps. In contrast to the previous metal catalysts, B,F-doped g-C₃N₄ (CNBF) materials are highly selective oxidation catalysts for cyclohexanone and do not produce any adipic acid or valeric acid under these conditions (Scheme 13).



Scheme 13. Selective oxidation of cyclohexane to cyclohexanone.

Using CNBF-0.3 as catalyst in acetonitrile, the total conversion of cyclohexane was 7.8% and the selectivity towards cyclohexanone was as high as 91% after 4 h. Interestingly, the CNBF-1.0 catalyst afforded 100% selectivity towards the formation of cyclohexanone, although the conversion of cyclohexane was lower than observed for CNBF-0.3 and CNBF-0.5 catalysts. GC-MS analysis showed that no over-oxidation byproduct was produced for all CNBF catalyzed reactions (Table 4, Entries 1-4).¹³⁹

Table 4. Conversion and selectivity of cyclohexane oxidation over CNBF catalysts and GSCN catalysts, adapted from Ref.^{139, 126}.

Entry	Catalyst	Total Conversion [%]	Sel. for one [b]	Sel. For ol ^[b]
1 ^a	g-C ₃ N ₄	1.6	>99	---
2 ^a	CNBF-0.3	7.5	91	9
3 ^a	CNBF-0.5	7.8	89	10.6

4 ^a	CNBF-1.0	5.3	>99	---
5 ^b	g-C ₃ N ₄	0	---	---
6 ^b	GS (20 mg)	0	---	---
7 ^b	g-C ₃ N ₄ +GS	0	---	---
8 ^b	GSCN-2.5	2	84	16
9 ^{bc}	GSCN-12.5	11	67	---
10 ^b	GSCN-20	12	94	6
11 ^b	GSCN-50	3	87	13

^a No products were detected without the carbon nitride catalyst. Reaction conditions: cyclohexane 0.8 mL, H₂O₂ (30% in water solution) 0.51 mL, catalyst 50 mg, temperature 150 °C, 4 h. ^b Typical conditions: 10 mL of CH₃CN, 10 mmol of cyclohexane, 50 mg of catalyst, O₂ (10 bar), 150 °C, 4 h. ^c Caprolactone (23%) was detected.

A synergistic effect of graphene sheet (GS) and g-C₃N₄ on promoting the catalytic activation of molecular oxygen was observed by Li *et al.* via the synthesis of GS/G-C₃N₄ composite,¹²⁶ which was not found for the physical mixture of them (Table 4, Entries 7). Low conversion (2-3%) was achieved by GSCN-2.5 (GSCN-x, x refers to the weighed-in amount of GS per batch) and GSCN-50 samples with too little or too much GS. GSCN-12.5 provided a conversion (11%) of cyclohexane with a moderate selectivity (67%) to cyclohexanone. GSCN-20 gave a good conversion (12%) and a high selectivity (94%) toward cyclohexanone. No over-oxidation byproducts, such as adipic acid or valeric acid, were detected in the GC-MS analysis for all the reactions, demonstrating that the selective C-H oxidation is provided from the HOMO of the catalytic dyad of GS layers and g-C₃N₄ layers in a synergistic fashion. The composite is also applicable for other secondary C-H bond of other extended substrates.¹²⁶

A series of metal-doped graphitic carbon nitride catalyst (Fe-, Co-, Ni-, Mn-, and Cu-g-C₃N₄) were synthesized via heating dicyandiamide with metal chloride by Wang and coworkers.¹⁴⁰ Significant activity improvement for benzene to phenol over

Fe-g-C₃N₄ and Cu-g-C₃N₄ was observed both with and without visible light. That was attributed to that the modified g-C₃N₄ could greatly improve the decomposition rate of the oxidant (H₂O₂). The optimal yield of phenol was 4.8 % with 100% selectivity over Fe-g-C₃N₄ under visible light. After being modified with SBA-15, the yield could be advanced to 11.9%. The Fe-g-C₃N₄ and Co-g-C₃N₄ also offered enhanced conversion and selectivity for the oxidation of styrene with O₂, especially in the presence of visible light. Similar type of metal-g-C₃N₄ (Cu-, Fe-, V-, Co-, and Ni-g-C₃N₄) was developed by Jiang & Han *et al.* via co-pyrolysis of urea and the metal salt.¹⁴¹ Vanadium doped graphitic carbon nitride catalyst (V-g-C₃N₄) was found to be the most efficient catalyst for the direct synthesis of phenol from benzene. Using H₂O₂ as the oxidant, 18.2 % yield of phenol was obtained with the selectivity of 100 % under optimized conditions. The V-g-C₃N₄ demonstrated good stability and could be reused for more than four times without significant activity loss. Very recently, a dual-catalysis by non-noble metal system by simultaneously using C₃N₄ and Keggon-type polyoxometalate H₅PMo₁₀V₂O₄₀ (PMoV₂) as catalysts, denoted as C₃N₄-PMoV₂, was applied to the reductant-free aerobic oxidation of benzene to phenol.¹⁴² This system avoided the use of expensive noble metals and wasteful sacrificial reducing agents, developing a so-called “dream oxidation” system. By using LiOAc as an effective additive, a maximum phenol yield of 13.6% was achieved in a 50 vol.% aqueous solution of acetic acid under 2.0 MPa O₂, 130 °C for 4.5 h reaction time. A dual-catalysis mechanism was proposed: benzene was activated on the melem unit of C₃N₄ and O₂ by the V-O-V structure of PMoV₂ (Figure 1).

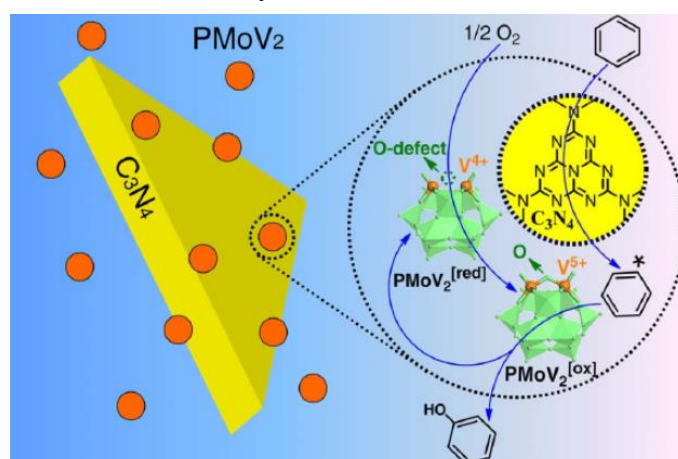


Figure 1. Proposed mechanism pathway for C₃N₄-PMoV₂-catalyzed aerobic oxidation of benzene to phenol. Reprinted with permission from Ref.¹⁴². Copyright © 2014, Rights Managed by Nature Publishing Group.

2.2.2 By Metal@g-C₃N₄ (g-C₃N₄ as the support)

Although suffering from the disadvantages of relatively high cost and toxicity, there is no doubt that noble metal-containing catalysts are always the most effective catalysts for a variety of reactions. Catalysts comprised of noble metal nanoparticles (i.e. Au, Pd, Pt) and a support are of the most attractive ones in both laboratory studies and industrial applications because they have shown potentials of possessing comparable catalytic performance with homogeneous catalysts and convenient recycling steps as heterogeneous catalysts. The catalytic activity is related to the nature of both the metal and the support chosen. The support acts not only as a platform for the dispersion of active species (ASs) and for the catalytic reaction, but also as the assistant impacting the performance. It provides active sites at the metal-support boundary, and influences the redox state of the metal nanoparticles. Some supports themselves also afford active sites. G-C₃N₄ can be chemically shaped to a variety of nanostructures and is of high chemical and thermal stability, possessing the essential requirements for catalyst supports. The nitrogen functionalities on the surface might act as strong Lewis base sites, while the π -bonded planar layered configurations are expected to anchor the substrate. Therefore, g-C₃N₄ is a fascinating choice of catalyst support for heterogeneous catalysts.

Prati *et al.* immobilized Pd nanoparticles on bulk g-C₃N₄ and subjected it to the oxidation of benzyl alcohol.¹⁴³ For comparison, the other two nitrogen-doped porous polymer networks were also selected as the particle carrier. The two networks were synthesized by polymerization of *para*-dicyanobenzene (CTF_{DCB}) and 2,6-dicyanopyridine (CTF_{DCP}) in the presence of ZnCl₂, respectively. All the three catalysts showed better performance than Pd/C with the following activity order: Pd/C₃N₄>Pd/CTF_{DCP}>Pd/CTF_{DCB}. TOF as high as 14131(molPd)⁻¹h⁻¹ was achieved in the case of Pd/C₃N₄ under 80 °C, 1 atm O₂ (Table 5). Designed experiments showed

that the activity did not correlate to the Pd size, oxidation states, the surface areas or the acidic/basic properties of these catalysts.

Table 5. Oxidation of benzyl alcohol by using supported Pd catalysts,^a adapted from Ref.¹⁴³.

Catalyst	Converted (molPd) ⁻¹ h ⁻¹	Selectivity ^b				
		Toluene	Benzaldehyde	Benzoic acid	Benzyl benzoate	Unknown
Pd/CTF _{DCB}	4917	31	66	1	1	1
Pd/CTF _{DCP}	8025	26	71	1.5	1	0.5
Pd/C ₃ N ₄	14131	35	62	0.5	2	0.5

^a Reaction conditions. Alcohol/metal: 5000, T=80 °C, P_{O₂} =2 atm, benzyl alcohol/cyclohexane ratio 50:50. ^b Selectivity calculated at 90% conversion as mol of products (mol converted)⁻¹*100.

The activity changes were in line with the nitrogen content of the three supports (Figure 2). An indication of the impact of nitrogen-containing groups has been revealed by studying the changes in the nitrogen functionality of the catalyst compared to the original support material by means of XPS. For both CTF_{DCP} and C₃N₄ support materials, there is a decrease in C₃N functionality with the addition of Pd. This strongly indicates that the Pd associates with these sites. Furthermore, a distinct decrease in N (from 57% to 28%) determined by XPS in the case of C₃N₄ before and after Pd deposition strongly verified the fact that a more relevant coordination of Pd on N groups may contribute to a better catalytic activity.

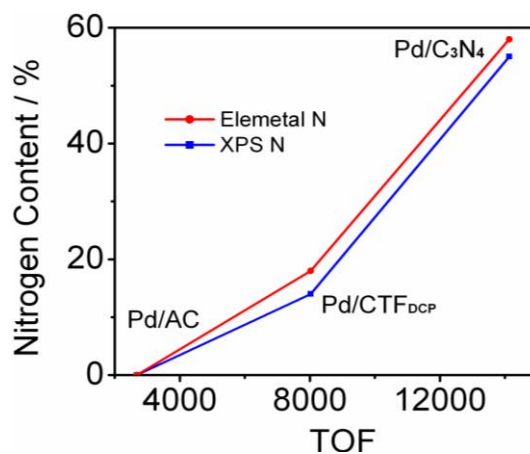


Figure 2. Activity of the catalyst as a function of the nitrogen concentration, adapted from Ref.¹⁴³.

Besides the investigation of increasing catalytic activity in the oxidation reactions, intensive interests have also been on studying the mechanism of the oxidation reactions which often include a step of oxygen activation. It is generally believed that the activation of molecular oxygen takes place on the defects or oxygen vacancies,¹⁴⁴ but it is hard to find out whether the activated oxygen species come from the metal or the oxygen site as catalysts used for oxidation reactions contain oxygen themselves. C_3N_4 , with its matrix containing only N and C without oxygen, offers great opportunities for clarifying the mechanism of oxygen activation, inspiring research interests recently.¹⁴⁵⁻¹⁴⁶ Zhu *et al.* reported an investigation of $Au@C_3N_4$ and $Fe@C_3N_4$ were inactive for gas phase CO oxidation at temperatures below 300 °C or liquid phase oxidation of benzyl alcohol with molecular oxygen as the oxidant.¹⁴⁵ However, Au supported on activated carbon catalysts were shown to be active for the liquid oxidation. Conclusions were drawn that the inactivity of C_3N_4 based catalysts were due to the lack of oxygen absorption/activation sites such as oxygen vacancies on the support whereas oxygen from activated carbon supports interacts with oxygen to activate it for the oxidation reaction through a defect formation/removal process. They recently applied $g-C_3N_4/SBA-15$ composites as catalyst support for Au and Pt nanoparticles and the prepared catalysts were subjected to CO oxidation.¹⁴⁷ Compared to using SBA-15 as the support, $Pt@g-C_3N_4/SBA-15$ afforded much higher activity with a lower ignition temperature for CO oxidation due to the small particle size, high dispersion, and possibly new electronic properties caused by the interaction with $g-C_3N_4$. In contrast, $Au@g-C_3N_4/SBA-15$ showed no activity, and no change in activity was observed compared to the pure support. The low activity was ascribed to the absence of oxygen-containing species on $g-C_3N_4$, which was regarded as the O_2 activation sites.^{145, 148-149} For $Pt@g-C_3N_4/SBA-15$, partially oxidized Pt particles could offer the oxygen species while no oxidized Au were observed on $Au@g-C_3N_4/SBA-15$. However, a report by Gabriel *et al.* concluded that the inactivity of C_3N_4 based Au catalysts was attributed to the lack of basic surface OH

groups, and these OH groups were supposed to be required to activate CO for the gas phase CO oxidation, pointing to a fundamentally different reason.¹⁴⁶

3. Catalytic hydrogenation by g-C₃N₄ supported metal nanoparticles

As discussed above, carbon nitride meets all the requirements as a support material for heterogeneous catalysts. Pd@C₃N₄ has been the most investigated supported precious metal catalyst now in the hydrogenation of organic chemicals since its first use for phenol hydrogenation.^{70, 150-153}

3.1 Phenol hydrogenation

The one-step, selective direct hydrogenation of phenol is certainly a preferable process to produce cyclohexanone, as it avoids the endothermic dehydrogenation step.¹⁵⁴ Liquid phase hydrogenation can be of great interest since the reaction can be performed at relatively low temperatures, avoiding problems like coking in gas-phase reactions. However, cyclohexanone is an active intermediate and is easily hydrogenated to cyclohexanol and other byproducts. It seems that Pd is usually the metal of choice for this conversion due to its low activity for the hydrogenation of aliphatic or cycloaliphatic ketones than other noble metals.^{1,155} The catalytic activity of Pd catalysts can be controlled by varying the support material (MgO, Al₂O₃, activated carbon, TiO₂, MCM-41, mpg-C₃N₄).¹⁵² Indeed, for the vast majority of Pd catalysts, the hydrogenation of cyclohexanone is inevitable, especially at high conversions. As a consequence, complete production of cyclohexanone at approximating full conversion is the apex of phenol hydrogenation.

One study opened the field of taking g-C₃N₄ as support for the liquid hydrogenation of phenol. Highly-dispersed Pd nanoparticles were introduced as a functional moiety into a mpg-C₃N₄ framework (Figure 3).⁷⁰ All the Pd particles were about 3 nm in size, well-separated from each other. The hybrid material, Pd@mpg-C₃N₄, was subsequently used as a catalyst for the hydrogenation of phenol.

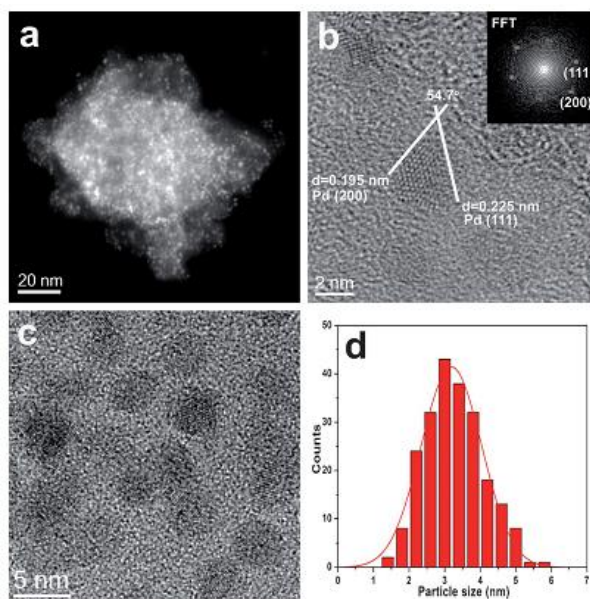
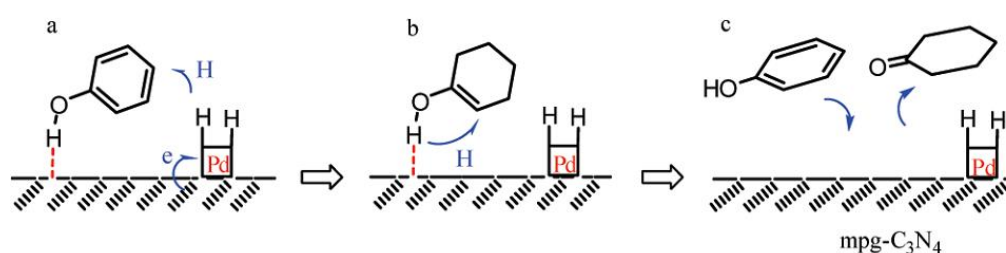


Figure 3. STEM (a), HRTEM (b), TEM (c), and particle size distribution (PSD) (d) of Pd@mpg-C₃N₄. Inset in (b): local fast Fourier Transform (FFT). Reprinted with permission from Ref. ⁷⁰. Copyright © 2011, American Chemical Society.

Prior research on the one-step hydrogenation of phenol to cyclohexanone showed that cyclohexanone was easily further hydrogenated to cyclohexanol, and achieving high selectivity (>95%) at elevated conversion (>80%) is a great challenge.^{78, 154, 156} Pd@mpg-C₃N₄ was shown to be highly active to promote the selective formation of cyclohexanone even under an atmospheric pressure of hydrogen and under aqueous conditions. For example, the catalytic hydrogenation of phenol with 5 mol% Pd@mpg-C₃N₄ in water at 65 °C proceeded with 99% conversion in 2 h and more than 99% selectivity for cyclohexanone. The observed reaction rates were generally much higher than those obtained with a classical Pd@C complex which also gave low selectivity toward cyclohexanone in general and required the use of additives. Significantly, the Pd@mpg-C₃N₄ catalyst was successfully applied to other hydroxylated aromatic compounds with both high conversion and selectivity (>99%). The high activity and selectivity resulted from the nature of mpg-C₃N₄. The rich nitrogen atoms supply anchoring sites for metal particles which stabilize the particles and the electron transfer from carbon nitride to Pd particles promotes the hydrogen dissociation (Scheme. 14a). Phenol can interact with the surface through the hydroxyl group to form strong O-H...N or O-H... π interactions. As a basic host, mpg-C₃N₄

favors the nonplanar adsorption of phenol because the O-H... π interaction is weaker. Therefore, the reaction mechanism is proposed as Scheme 14. In the initial stage, phenol can be easily absorbed on the surface of the catalyst, and H₂ is activated by the electronically supported Pd (Scheme 14a). The benzene ring of phenol is then partially hydrogenated to the enol (Scheme 14b), which can isomerize rapidly to give cyclohexanone. There is only a weaker H-bridge donor, and the cyclohexanone leaves the surface of the catalyst quickly, being replaced by a more strongly binding new phenol molecule (Scheme 14c) and avoiding further hydrogenation to cyclohexanol.



Scheme 14. Possible reaction mechanism of phenol over Pd@mpg-C₃N₄. Reprinted with permission from Ref.⁷⁰. Copyright © 2011, American Chemical Society.

For detailed information about the reasons of the highly active catalytic activity and high selectivity of Pd@mpg-C₃N₄, further studies were performed to investigate the kinetics of the process.¹⁵² By Arrhenius plots, the activation energy (E_a) in the case of Pd@mpg-C₃N₄ was calculated to be 35.9 kJ mol⁻¹ in aqueous phase,¹⁵² less than 48 kJ mol⁻¹ of traditional Ni-ZSM-5 in vapor phase,¹⁵⁷ which is responsible for the better activity. DFT calculations showed that the free energy barrier of the transition state could be lowered by water, which explained the higher catalytic activity in aqueous phase than in organic phase. The H₂ activation theory was proved by the isotopic tracing experiment. Adsorption experiments of mpg-C₃N₄ towards phenol and cyclohexanone showed that the carbon nitride with NH and NH₂ exhibited superior performance for the adsorption of phenol with a high absorption capacity, almost 20 times than that of cyclohexanone (Figure 4). It validated the theory that the produced cyclohexanone tended to leave the catalyst after the hydrogenation of phenol to cyclohexanone, which contributed to the high selectivity towards cyclohexanone.⁷⁰

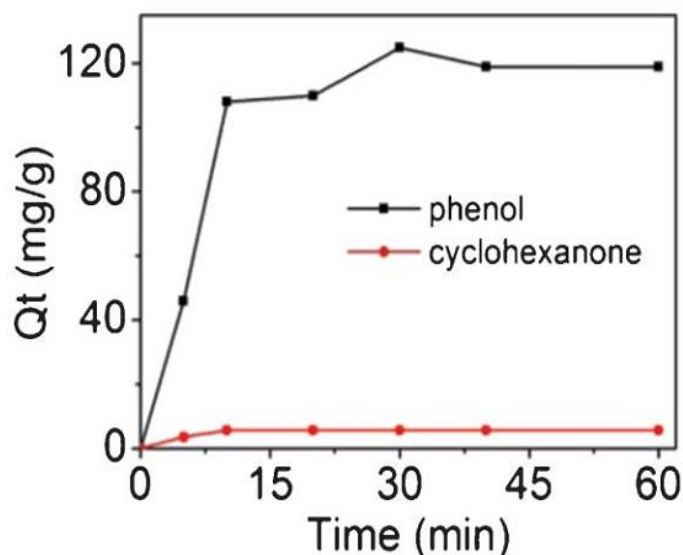
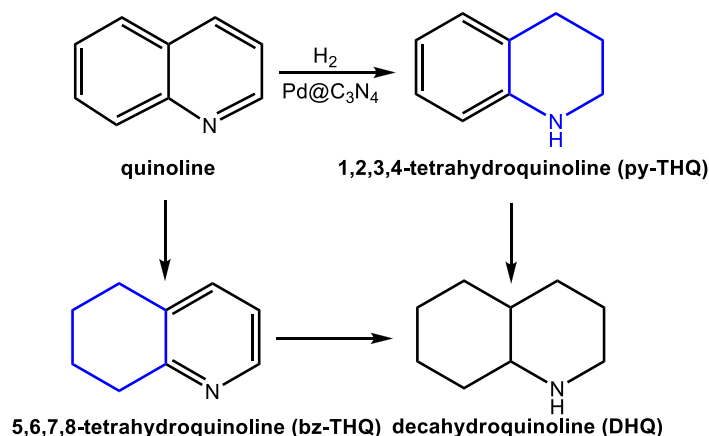


Figure. 4 Comparison of the phenol and cyclohexanone adsorption capacity over $\text{mpg-C}_3\text{N}_4$,¹⁵² reproduced by permission of The Royal Society of Chemistry.

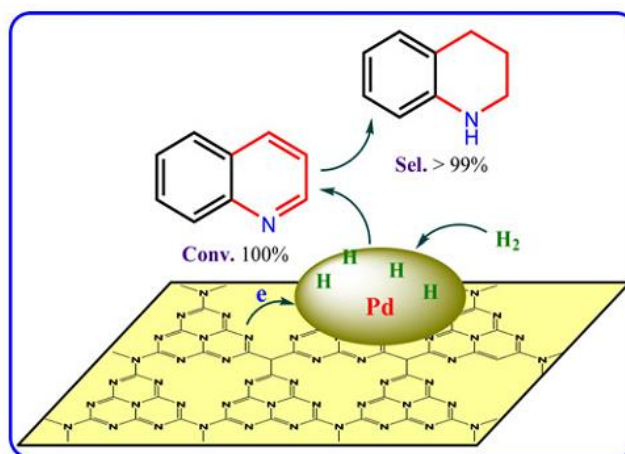
3.2 Quinoline Hydrogenation

$\text{Pd@mpg-C}_3\text{N}_4$ also showed excellent catalytic performance for the selective hydrogenation of nitrogen heterocycles.¹⁵¹ 1,2,3,4-tetrahydroquinoline (THQ) is an important intermediate for the synthesis of drugs, agrochemicals, dyes, alkaloids, and many other biological active molecules¹⁵⁸⁻¹⁵⁹ Direct selective hydrogenation of quinoline is widely regarded as the most convenient and most promising way owing to its high atom utilization together with easy access of the raw material. The core task of active supported Pd catalysts is preventing the formation of excessive hydrogenation product, decahydroquinoline (DHQ) (Scheme 15).



Scheme 15. Reaction pathways for quinoline hydrogenation, reproduced with permission from Ref.¹⁵¹. Copyright © 2012 Elsevier Inc. All rights reserved.

The Pd@mpg-C₃N₄ provided full conversion and >99% selectivity for THQ under 1 bar of H₂ and low temperatures, which was much higher than Pd/C at the same reaction conditions.¹⁵¹ The high activity originated from the electronic effect between Pd nanoparticles and C₃N₄ (Scheme 16) while the high selectivity towards THQ derived from the prior adsorption of nitrogen-containing aromatic ring on the support. The texture of the g-C₃N₄ also influenced the activity of the reaction. Ordered mesoporous C₃N₄ (ompg-C₃N₄) replicated by SBA-15 showed better performance as the support than the disordered one (mpg-C₃N₄) replicated by Ludox HS-40, which was attributed to the more favoring mass transfer. All the Pd particles were well dispersed and the size was narrowly distributed with a mean size of 4.09 nm. The Pd species existed mainly in the form of Pd⁰ (70%) which was widely regarded as the active site. The Pd@ompg-C₃N₄ also promoted the selective hydrogenation of substituted quinolines, and even oxygen heterocyclic compounds with high selectivity.

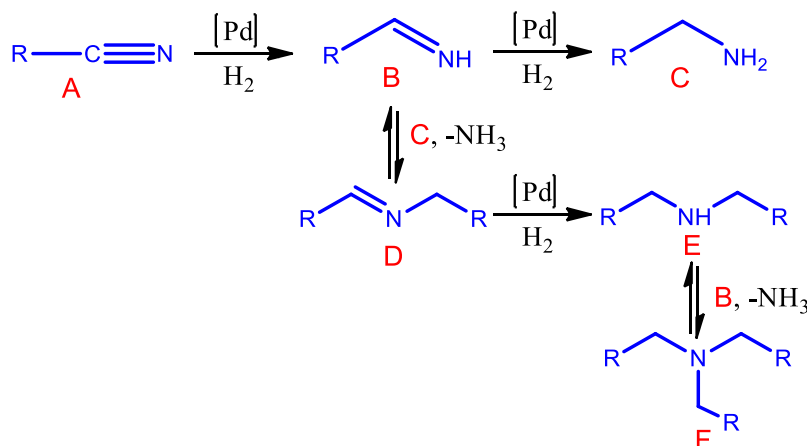


Scheme 16. The hydrogenation of quinoline to THQ over Pd@C₃N₄, reproduced with permission from Ref.¹⁵¹. Copyright © 2012 Elsevier Inc. All rights reserved.

3.3 Nitriles Hydrogenation

Hydrogenation of nitriles is one of the most common methods to prepare amines due to the high atom efficiency.¹⁶⁰⁻¹⁶⁴ The liquid hydrogenation of nitriles occurs as a set of consecutive and parallel reactions owing to the high reactivity of the intermediates (Scheme 17), resulting in a mixture of primary, secondary and tertiary amines.¹⁶⁰ Separation of the reaction products is usually difficult, due to small

differences in boiling point. For this reason, one of the most important issues in the hydrogenation of nitriles is the selectivity control.



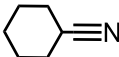
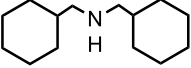
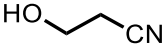
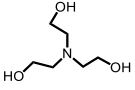
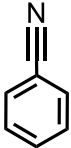
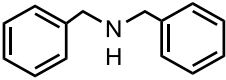
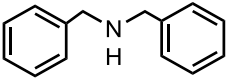
Scheme 17. Formation of primary, secondary, and tertiary amines in the catalytic hydrogenation of nitriles, reproduced with permission from Ref. ¹⁵⁰. Copyright © 2012 Elsevier B.V. All rights reserved.

Pd@mpg-C₃N₄ was employed for the hydrogenation of butyronitrile (BTN) under benign conditions.¹⁵⁰ In solvent-free conditions, the reaction gave 100% conversion of BTN and 99% selectivity of tri-n-butylamine (TBA) after 9 h over Pd@mpg-C₃N₄. The conversion of BTN increased from 70 to 99% by increasing the pressure from 0.1 MPa to 3 MPa at 70 °C for 2 h. No side product was observed even under high temperature and high hydrogen pressure.

The application of Pd@mpg-C₃N₄ on different nitriles was also exploited (Table 6). The acetonitrile furnished 99% conversion with 99% selectivity toward triethylamine (Table 6, entry 1) at 70 °C in 6 h, whereas aromatic benzonitrile provided 89% conversion with 99% selectivity (Table 6, entry 6). The hydroxyl substituted 3-hydroxypropionitrile offered a moderate conversion (40%) and selectivity (73%). However, no product was detected in the case of chloro-substituted 4-chlorobutyronitrile. Moreover, the Pd@mpg-C₃N₄ was compared with the commercially available Pd@C, and the home made Pd@TiO₂, Pd@CeO₂, and Pd@γ-Al₂O₃, for the hydrogenation of benzonitrile at 0.1 MPa of hydrogen and 80 °C for 12 h. Results from Table 6 clearly show that the Pd@mpg-C₃N₄ catalyst affords

better activity and selectivity than the commercially prepared Pd/C and Pd on other supports.

Table 6. Scope and limitations of Pd@mpg-C₃N₄ and comparative catalytic performance of different palladium catalysts,^a adapted from Ref.¹⁵⁰.

Entry	Substrate	T °C	Conv. %[%]	Product	Sel. [%]
1		70	99		>99
2		70	99		>99
3		100	70		>99
4 ^b		80	40		73
5 ^c		80	---	---	--
6		80	89		>99
7 ^d		80	35		>99
8 ^e		80	25		85
9 ^f		80	32		94
10 ^g		80	16		88
11 ^h		80	15		93

^a 10 mmol substrate, Pd@mpg-C₃N₄ (0.2% mol Pd relative to substrate), 1.0 MPa H₂, reaction time 6 h.

^b 10 mmol 3-hydroxypropionitrile, Pd@mpg-C₃N₄ (0.2% mol Pd relative to substrate), 0.1 MPa H₂, reaction time 12 h.

^c 10 mmol 4-chlorobutyronitrile, other reaction conditions as in entry 4.

^d 10 mmol benzonitrile, other reaction conditions as in entry 4.

^e commercial Pd/C as catalyst, other reaction conditions as in entry 4.

^f Pd/TiO₂ as catalyst, other reaction conditions as in entry 4.

^g Pd/CeO₂ as catalyst, other reaction conditions as in entry 4.

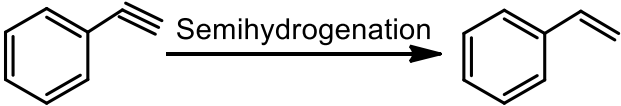
3.4 Alkyne and Alkene Hydrogenation

The synthetic potential and utility of alkynes in manufacture of fine chemicals is largely attributed to the formation of new carbon-carbon bonds by alkylation

combined with selective hydrogenation of the triple bond opening up routes both to alkanes by complete saturation and to alkenes by semi-hydrogenation.¹⁵⁵ The semi-hydrogenation of alkynes is a powerful tool to synthesize Z-alkenes which is an important building block of fine chemicals such as bioactive molecules, flavors and natural products.¹⁶⁵⁻¹⁶⁶ Palladium was basically chosen as the catalytic center because of its specific dissociation power for hydrogen gas. The deep hydrogenation is the same problem faced with because alkene is active over Pd catalysts. The choice of appropriate support is an alternative way to settle this issue.

A study indicated that Pd@mpg-C₃N₄ could hydrogenate phenylacetylene to styrene with outstanding selectivity even at high conversions.¹⁵³ 94 % selectivity was still remained at full conversion within 85 min. Notably, Au-Pd@mpg-C₃N₄ gave better selectivity of 96 % but with low conversion. Although Lindlar catalyst demonstrated the best selectivity approximating 100 %, only 5 % of phenylacetylene was hydrogenated even after 270 min of reaction (Table 7).

Table 7. Hydrogenation of phenylacetylene catalyzed by various catalysts, adapted from Ref.¹⁵³



Entry	Catalyst	Time [min]	Conv. ^b [%]	Sel. ^b [%]
1 ^c	Pd@carbon	15	85	88
2 ^d	Pd@mpg-C ₃ N ₄	85	>99	94
3 ^d	2.5Au-Pd@mpg-C ₃ N ₄	60	29	96
4 ^d	Pd@γ-Al ₂ O ₃	45	>99	90
5 ^e	Pd@TiO ₂	20	100	86-90
6 ^d	Pd@MgO	105	>99	91
7 ^d	Pd@CeO ₂	150	95	91
8 ^f	Lindlar catalyst	270	5	>99
9 ^g	Pd@mpg-C ₃ N ₄	60	17	97

^a Reaction conditions: 10 mg catalyst, 5.85 mmol phenylacetylene, 50 mL ethanol, 303 K, atmospheric H₂ bubbling. ^b Analysed by GC. ^c Data taken from reference, 1 wt% Pd, 0.2 MPa H₂ and 323 K. ^d 5.64 wt%Pd. ^e Data taken from reference, 1 wt% Pd, 5 bar H₂ and 303 K. ^f 1 wt%Pd, provided by NHU company. ^g 0.67 wt% Pd.

Carbon nitride nanotubes (CN) was developed by Song and coworkers.¹⁶⁷ The CN was synthesized by using AAO membrane as a template and ethylenediamine /carbon tetrachloride (CCl_4) as precursors. Then Pd or Pt ions were reduced on the tubes by NaBH_4 with excellent dispersion. The 20%Pt/CN was then subjected to the gas phase hydrogenation of cyclohexene. The conversion of the cyclohexene was approximately 100% in the temperature range of 15 to 200 °C. As the reaction temperature increased, the yield of cyclohexane decreased for its dehydrogenation reaction and benzene appeared (Figure 5a). TEM image of the 20%Pt/CN after the reaction showed that the size of the Pt nanoparticles remained in high dispersion (Figure 5b).

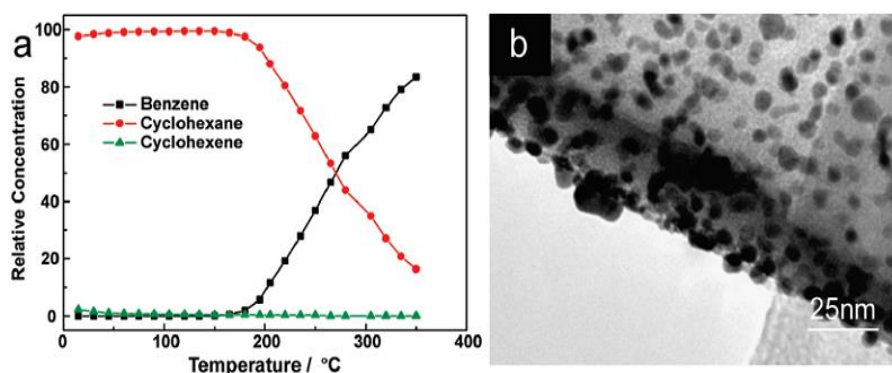


Figure 5. (a) The catalytic ability of the 20 wt%Pt/CN at different temperatures and (b) the TEM image of used 20 wt%Pt/CN. Reprinted with permission from Ref.¹⁶⁷.

Copyright © 2009, American chemical Society.

3.5 Reduction of nitro compounds

Besides hydrogenation of nitriles, the hydrogenation of nitro compounds provides a feasible way to the production of corresponding amines.¹⁵⁵ One recent publication described the hydrogenation of 4-nitrophenol to 4-aminophenol by mesoporous $\text{g-C}_3\text{N}_4$ nanorods (m-CNR) supported noble metal catalysts (Au, Pt, Pd).¹⁶⁸ The ultrafine noble metal NPs were homogeneously distributed inside the mesochannels (Figure 6).

The Au@m-CNR, Pd@m-CNR and Pt@m-CNR were tested in the hydrogenation of nitrophenol by a strong reducing agent, NaBH_4 . All these catalysts demonstrated high conversions above 96% due to the high activity of the ultrafine

NPs and the enhanced mass transfer within the short and open nanochannels of m-CNR, and most importantly, the catalysts eliminated the shortcoming of bad reusability of non-supported or SBA-15-supported Pt catalyst. No obvious morphology change was observed for both the metal particles and the support, which accounts for the good reusability.

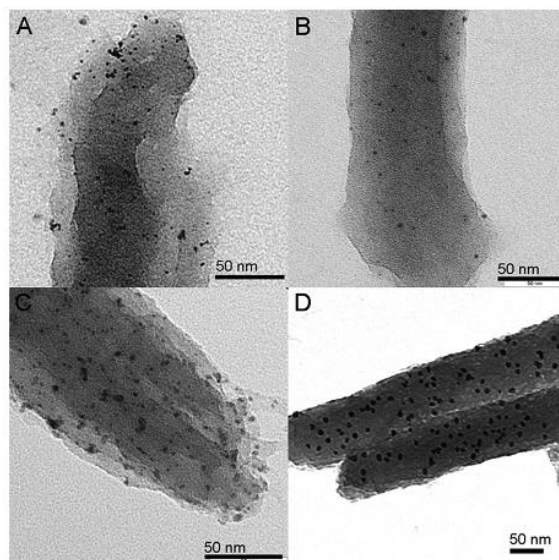


Figure 6. TEM images of m-CNR-Pt-2 nm (A), m-CNR-Au-2 nm (B), mCNR-Pd-3 nm (C), and m-CNR-Au-9 nm (D),¹⁶⁸ reproduced by permission of The Royal Society of Chemistry.

In addition to the role of a support, g-C₃N₄ itself is a photocatalyst which can trigger water splitting under light illumination.^{68, 169} Therefore, Pt@g-C₃N₄ was taken as a multifunctional catalyst for hydrogenation by *in situ* production of H₂ by using triethanolamine (TEA) as a sacrificial electron donor under illumination with a 300 W Xe lamp. The conversion of 85% was achieved and not changed when the reaction was conducted under N₂ atmosphere. And no reaction took place in the dark or without catalyst, suggesting that the Pt@m-CNR indeed served as a tandem catalyst.

A carbon nitride containing catalyst for hydrogenation of nitro compounds were designed in a completely different way by Ding and coworkers.¹⁷⁰ This specially designed catalyst possessed a unique structure composed of carbon nitride (CN) with underlying nickel supported on Al₂O₃ (Scheme 18). The pure CN was inert for hydrogenation without the help of nickel while the Pd/Al₂O₃ showed no activity for

the hydrogenation in strong acidic conditions. In contrast, the CN/Ni/Al₂O₃ composite revealed good performance for hydrogenation of nitro compounds under strong acidic conditions, including the one-step hydrogenation of nitrobenzene in 1.5 M H₂SO₄ to produce 4-aminophenol (Scheme 18). Characterization demonstrated that the nickel in the catalyst was in an electron-deficient state because some of its electron had been donated to CN (HRTEM, PES); thus, the hydrogen could be directly adsorbed and activated by the CN (HD exchange, in situ IR and NMR). The specific structure avoided the direct contact of the active Ni with the strong acidic condition, leading to good stability and the inert CN was activated by the nickel for catalytic hydrogenation of nitro compounds.¹⁷⁰



Scheme 18. Schematic of the principle of the mesostructural CN catalyst with underlying nickel. The points are (1) electron donation from nickel to CN; (2) dissociative adsorption of the hydrogen molecule bonded to the CN; (3) reduction of the nitro compound by the activated hydrogen; (4) the adsorbed hydrogen is capable of hydrogenation under strong acidic conditions, with concentrated protons taking part in the reaction for the rearrangement of the intermediate; and (5) nickel is protected from corrosion or poisoning. Reprinted with permission from Ref.¹⁷⁰.

Copyright © 2014, American Chemical Society.

3.6 Hydrogenation of olefins and unsaturated biomass

Compared with gaseous hydrogen, stable liquid hydrogen source (*e.g.*, formic acid) in principle is characterized by better handleability. Li and Chen *et al.* proposed the first transfer hydrogenation case over metal@mpg-C₃N₄ (M = Ag, Au, Pd and Pt) dyads.¹⁷¹ These Mott-Schottky catalysts were subjected to the hydrogenation of styrene to ethylbenzene. Pd@mpg-C₃N₄ was the only effective combination. The total conversion of styrene to ethylbenzene was achieved when three equivalents of FA or more were used. The reduction of styrene could not proceed in the absence of catalyst or FA (Table 8, Entries 1, 6). The solvent screening survey showed that water, CH₃CN and acetic ester provided the same outcome, which is better than ethanol, DMF and THF (Table 8, Entries 13-17). The smooth reaction in water made the Pd@g-C₃N₄/formic acid system meet the requirements of green chemistry.

Table 8. Study of the reaction conditions,^a adapted from Ref.¹⁷¹.

Entry	Catalyst	Solvent	C. ^b [%]	S. ^b [%]
1	---	H ₂ O	---	---
2	Pt@mpg-C ₃ N ₄	H ₂ O	Trace	---
3	Au@mpg-C ₃ N ₄	H ₂ O	---	---
4	Ag@mpg-C ₃ N ₄	H ₂ O	---	---
5	Pd@mpg-C ₃ N ₄	H ₂ O	>99.9	>99.9
6 ^c	Pd@mpg-C ₃ N ₄	H ₂ O	---	---
7 ^d	Pd@mpg-C ₃ N ₄	H ₂ O	>99.9	>99.9
8 ^e	Pd@mpg-C ₃ N ₄	H ₂ O	---	---
9 ^f	Pd@N-LC	H ₂ O	---	---
10	Pd@SiO ₂	H ₂ O	4.44	>99.9
11	Pd ²⁺ @mpg-C ₃ N ₄	H ₂ O	---	---
12	mpg-C ₃ N ₄	H ₂ O	---	---
13	Pd@mpg-C ₃ N ₄	Ethanol	57.98	>99.9
14	Pd@mpg-C ₃ N ₄	CH ₃ CN	>99.9	>99.9
15	Pd@mpg-C ₃ N ₄	Ethyl acetate	>99.9	>99.9
16	Pd@mpg-C ₃ N ₄	DMF	32.70	>99.9

17	Pd@mpg-C ₃ N ₄	THF	76.02	>99.9
----	--------------------------------------	-----	-------	-------

^a Standard conditions: 2.5 mL of H₂O, 0.1 mmol of styrene, 0.3 mmol of FA, 10 mg of catalyst, 15 min, T= 298 K. ^b Conversions (C.) and selectivity (S.) were determined by GC by using a FID detector. ^c Without FA. ^d The reaction was conducted in N₂. ^e CB: carbon black. ^f N-LC: Nitrogen-doped layered carbon.

Then, Pd@mpg-C₃N₄ was also evaluated for the hydrogenation of 2-methylfuran to 2-methyltetrahydrofuran (MTHF), which is the key step for increasing the hydrogen/carbon ratios and thus transforming the biomass (furfural) to renewable biofuel (MTHF). The transfer hydrogenation of the conjugated diene turned out to proceed with high yield which far exceeded that over Pd@N-LC, Pd@SiO₂, and Pd@C. The superb catalytic activity of Pd@mpg-C₃N₄ was attributed to the Mott-Schottky effect between the noble metal particles and the mpg-C₃N₄. The catalyst showed excellent reusability and stability in the reactions. A variety of C=C bonds was successfully hydrogenated in good yield over Pd@mpg-C₃N₄/formic acid system, demonstrating the generality of the catalytic system.

3.7 Hydrogenation of carbon dioxide

As aforementioned in section 3.6, formic acid is a nontoxic stable liquid hydrogen source. It has recently been recognized as a safe and reversible hydrogen storage material. H₂ can be liberated from FA even at room temperature (HCOOH→CO₂+H₂). From the perspective of H₂ storage, FA can be regenerated from the hydrogenation of carbon dioxide (CO₂+H₂→HCOOH). Pd@mpg-C₃N₄ was firstly demonstrated as a catalyst completing the CO₂ based hydrogen storage cycle by Yoon and coworkers (Scheme 19).¹⁷²



Scheme 19. Pd/mpg-C₃N₄ catalyzed hydrogen production and storage,¹⁷² reproduced by permission of The Royal Society of Chemistry.

For formic acid dehydrogenation, the Pd@mpg-C₃N₄ afforded a high TOF of 144 h⁻¹, which was higher than that of the multimetallic catalyst CoAuPd/C (TOF of 80 h⁻¹)¹⁷³ and comparable to the highest reported value (TOF of 158 h⁻¹) over AgPd/C.¹⁷⁴ The electron transfer from N into Pd was regarded responsible for the high activity. The Pd@ mpg-C₃N₄ also revealed its capability to synthesize formic acid with the aid triethylamine (avoiding the further reduction to methanol or methane). The formation of formic acid depended upon reaction conditions. A decrease in CO₂ pressure did not notably affect the quantity of formic acid while activity decreased under a lower H₂ pressure (Table 9, Entries 2, 3). Temperature also influenced the formic acid formation, and upon CO₂ hydrogenation at 150 °C, the formic acid yield increased significantly (Table 9, Entries 1vs.4 and 2vs.5). In this preliminary study, the best activity was observed upon utilization of the CO₂ and H₂ pressures of 13 bar and 27 bar, affording 4.74 mmol of FA (Table 9, Entry 5). Further decreases in CO₂ pressure, however, showed slightly reduced activities (Table 9, Entries 6, 7). Compared to the commercial Pd/C catalyst, an increased affinity of Pd/mpg-C₃N₄ toward CO₂ resulted in more than 2 times higher catalytic activity (Table 9, Entry 8). In the absence of Pd, no formic acid was formed (Table 9, Entry 9).

Table 9. CO₂ reduction catalyzed by Pd@mpg-C₃N₄,^a adapted from Ref.¹⁷².

Entry	Pressure ^b (bar)		Temp. (°C)	Formic acid ^c (mmol)
	CO ₂	H ₂		
1	20	20	100	1.74
2	13	27	100	1.70
3	27	13	100	1.22
4	20	20	150	3.62
5	13	27	150	4.74
6	10	30	150	4.26

7	5	35	150	3.44
8 ^d	13	27	150	2.05
9 ^e	13	27	150	n.d.

^a Mixtures of D₂O (10 mL), triethylamine (2.5 mL) and Pd/mpg-C₃N₄ (50 mg) were stirred for 24 h. ^b Pressure at 298 K. ^c Determined by ¹H NMR using acetone as an internal standard. ^d 10% commercial Pd/C was used as a catalyst. ^e mpg-C₃N₄ was used as a catalyst.

3.8 Hydrogenation of bromate

Bromate is one of the byproducts detected in drinking water from disinfection process involving ozonation of bromide-containing source waters.¹⁷⁵ Since bromate is a potential carcinogen to human beings, the World Health Organization (WHO) and the United States Environmental Protection Agency (USEPA) have recommended a maximum acceptable bromate concentration of 0.01 mg L⁻¹ in drinking water.¹⁷⁶ Liquid phase catalytic hydrogenation has been considered as one of the promising processes.¹⁷⁷ Chen *et al.* found that Pd supported on ordered mesoporous carbon nitride (MCN) exhibited much higher catalytic activity for the hydrogenation of bromate to bromide than Pd support on active carbon (AC) and CMK-3.¹⁷⁸ For example, the removals of bromate over Pd(2.01)/AC, Pd(2.09)/CMK-3 and Pd(2.20)/MCN-200 were 5.44%, 12.48% and 100%, respectively, after reaction for 50 min. The better performance was attributed to the mesoporous structure and the high IEP of MCN. The bromate hydrogenation process followed Langmuir-Hinshelwood model, indicating that the catalytic activity was related to the concentration of adsorbed bromate on the catalyst surface. The bromate reduction was a pH-dependent reaction and low pH favored bromate removal. A positive relationship between Pd particle size and TOF was observed, due to the enhanced H₂ solubility and the effective formation of β-PdH on large Pd particles. Moreover, the coexisting anions suppressed the reduction of bromate via the competitive adsorption with the bromate and the inhibition effect followed the order: CO₃²⁻ > SO₄²⁻ > HPO₄²⁻ > Br⁻ > NO₃⁻ > Cl⁻ > F⁻.

Among the reported applications of noble metal@g-C₃N₄ catalysts, enhanced activities, selectivities, and reusability were achieved in almost all cases. The catalytic activity enhancement were ascribed to two reasons: 1) the rich nitrogen atoms in g-C₃N₄ framework supplied perfect sites to anchor metal nanoparticles; on one hand, these sites could ensure the high dispersion of the NPs; on the other, the relatively strong interactions could prevent the NPs from leaching during the reaction.^{70, 143, 151} 2) the rich electrons of nitrogen atoms would transfer to Pd NPs and the Schottky barrier prevented the reverse electron flow from the metal to g-C₃N₄, which resulted in more effective electrons.¹⁷⁹ Attractively, the unique structural features of carbon nitride enable specific adsorption forms of organic compounds, thus offering advantages for high selectivity.^{70, 151}

4. Conclusion and Outlook

In this review, we have summarized the use of carbon nitride and its modifications in the use of oxidation and hydrogenation reactions and discussed the role of carbon nitride during the reaction processes. It is the peculiarities of carbon nitride as a semiconductor that make it a photocatalyst for these transformations. The rich nitrogen content and inherent chemical inertness and mechanical stability provide sufficient potentials for the employment of carbon nitride as metal-free catalysts and catalyst supports.

Based on these reported cases, intensified interest of applying carbon nitride as catalysts for other selective oxidation or hydrogenation reactions can be foreseen. To date, the systematic and clear mechanisms for the catalytic improvement are still desired. For photocatalytic oxidation, the catalytic performance is still far from perfect. The key issues still reside in reducing the band gap and improving the charge separation rate. The convincing mechanism for carbon nitride as photo-free oxidation catalysts is in desire. Thus the exploration of the real active site would be more meaningful. Although the carbon nitride shows great promotion for noble metal particles for oxidation and hydrogenation, where the improvement of activity and selectivity originates from remains a topic in debate. Better characterization of the interaction between g-C₃N₄ and the metal nanoparticles and the interaction between

g-C₃N₄ and the reactant would give a better understanding of these catalysts and provide guidance for catalyst designs.

To address these issues, lots of attempts are still needed. As a heterogeneous catalyst or support, the textual and morphological property is one of the most significant factors that influencing the catalytic performance. It determined the efficiency of mass transfer, the number of catalytic active sites and the morphology of the supported metal particles, *etc.* In photocatalytic reactions, the larger surface area and more developed porous structures would give rise to the light scattering and harvesting, leading to the higher light use efficiency.^{86, 89} However, most of the porous g-C₃N₄ materials applied in heterogeneous hydrogenation and oxidation are mainly prepared by hard-template methods which suffer from the drawbacks of high cost, tedious synthetic steps and pollution problems. The fabrication of carbon nitride with appropriate textual and morphological properties with easier soft-template or template-free strategies is still a great challenge and only a few successful examples are reported while the synthesized porous carbon nitrides are with limited specific surface areas.^{82, 139, 180} It's a meaningful research topic for not only the heterogeneous catalysis but the material science.

Heteroatom-doping would be another feasible method to adjust the catalytic ability of g-C₃N₄ based system by the variation of g-C₃N₄ electric properties, say the band structure. The change of the band structure would affect the optical properties of g-C₃N₄ as a metal-free catalyst and the Mott-Schottky effect as a support for metallic particles. Up to now, only a few successful examples concern the hydrogenation or oxidation of organic compounds and the theoretical calculation with respect to the doping effect is desired. The design of g-C₃N₄-based composites provides a promising way to tune the electric structure as well. Beyond that, the other components of the composite would reserve their original properties, affording the possibility of developing multifunctional catalyst or support for catalytic hydrogenation and oxidation. The search for well-performed catalysts for the degradation of dyes, water splitting and oxygen reduction reaction has boosted the development of g-C₃N₄ composites while these composites were seldom applied as catalysts or catalyst

supports in traditional catalytic oxidation and hydrogenation reactions. We believe that it would be a nice idea to develop g-C₃N₄-containing hybrids for hydrogenation and oxidation reactions.

G-C₃N₄ can bridge the gap between the visible light energy and some organocatalysts in photocatalytic oxidation. The photoelectrons from g-C₃N₄ can activate O₂ to •O₂⁻ and then the •O₂⁻ can activate the organocatalyst (*e.g.*, NHPI, IBA),¹⁰⁵⁻¹⁰⁶ which leads to the formation of a more active radical for oxidation. The exploration of new g-C₃N₄/organocatalyst combinations is now a promising however seldom touched area which should be attached more attention on.

The nitrogen atom forms in carbon nitride architecture are fixed according to the specific structure of carbon nitride, which has disadvantage to investigate the relevance between catalytic performance and the nitrogen form. Recently, a wider range of N-doped carbon materials have drawn considerable concerns.^{18, 27, 181-183} In these N-doped carbon materials, only minor parts of the carbon frameworks are replaced by nitrogen atoms. These CN_x has known to act as metal-free catalysts for oxygen reduction or catalyst support for hydrogenation reactions of biomass. Notably, the nitrogen content, the ratio of different nitrogen forms (*e.g.*, pyridinic N, pyrrolic N, quaternary graphitic N, amine N, *etc.*), and morphologies of CN_x materials can be easily tailored, demonstrating sufficient possibilities to access well-behaved catalysts. These CN_x would give more chances to establish corrections between the support structure and the catalytic performance.

Acknowledgements

Financial support from the National Natural Science Foundation of China (21376208&U1162124), the Zhejiang Provincial Natural Science Foundation for Distinguished Young Scholars of China (R13B030002), the Specialized Research Fund for the Doctoral Program of Higher Education (J20130060), the Fundamental Research Funds for the Central Universities, the Program for Zhejiang Leading Team of S&T Innovation, and the Partner Group Program of the Zhejiang University and the Max-Planck Society are greatly appreciated.

References

- 1 H. U. Blaser, A. Indolese, A. Schnyder, H. Steiner and M. Studer, *J. Mol. Catal. A-Chem.*, 2001, **173**, 3-18.
- 2 J. A. H. Dumesic, G. W.; Boudart, M., *Wiley-VCH Verlag GmbH & Co. KGaA: Weinheim*, 2008.
- 3 G. J. Hutchings, *J. Mater. Chem.*, 2009, **19**, 1222-1235.
- 4 L. Que and W. B. Tolman, *Nature*, 2008, **455**, 333-340.
- 5 A. Bouriazos, S. Sotiriou, C. Vangelis and G. Papadogianakis, *J. Organomet. Chem.*, 2010, **695**, 327-337.
- 6 R. J. Grau, A. E. Cassano and M. A. Baltanas, *Catal. Rev.*, 1988, **30**, 1-48.
- 7 V. Vaisarova, P. Svoboda, J. Soucek and J. Hetflejs, *Chem. Listy*, 1984, **78**, 737-757.
- 8 J. W. Veldsink, M. J. Bouma, N. H. Schoon and A. Beenackers, *Catal. Rev.*, 1997, **39**, 253-318.
- 9 R. A. Sheldon and J. Dakka, *Catal. Today*, 1994, **19**, 215-245.
- 10 R. A. Sheldon and R. S. Downing, *Appl. Catal. A-Gen.*, 1999, **189**, 163-183.
- 11 I. Arends and R. A. Sheldon, *Appl. Catal. A-Gen.*, 2001, **212**, 175-187.
- 12 T. Mallat and A. Baiker, *Chem. Rev.*, 2004, **104**, 3037-3058.
- 13 R. A. Sheldon, I. Arends and H. E. B. Lempers, *Collect. Czech. Chem. Commun.*, 1998, **63**, 1724-1742.
- 14 S. Carrettin, P. McMorn, P. Johnston, K. Griffin, C. J. Kiely and G. J. Hutchings, *Phys. Chem. Chem. Phys.*, 2003, **5**, 1329-1336.
- 15 C. Della Pina, E. Falletta, L. Prati and M. Rossi, *Chem. Soc. Rev.*, 2008, **37**, 2077-2095.
- 16 K. Mori, T. Hara, T. Mizugaki, K. Ebitani and K. Kaneda, *J. Am. Chem. Soc.*, 2004, **126**, 10657-10666.
- 17 A. Dhakshinamoorthy, M. Alvaro and H. Garcia, *Catal. Sci. Technol.*, 2011, **1**, 856-867.
- 18 X. Xu, Y. Li, Y. Gong, P. Zhang, H. Li and Y. Wang, *J. Am. Chem. Soc.*, 2012, **134**, 16987-16990.
- 19 V. V. Costa, M. Estrada, Y. Demidova, I. Prosvirin, V. Kriventsov, R. F. Cotta, S. Fuentes, A. Simakov and E. V. Gusevskaya, *J. Catal.*, 2012, **292**, 148-156.
- 20 A. Tanaka, K. Hashimoto and H. Kominami, *J. Am. Chem. Soc.*, 2012, **134**, 14526-14533.
- 21 D. I. Enache, J. K. Edwards, P. Landon, B. Solsona-Espriu, A. F. Carley, A. A. Herzing, M. Watanabe, C. J. Kiely, D. W. Knight and G. J. Hutchings, *Science*, 2006, **311**, 362-365.
- 22 Y. T. Chen, H. P. Wang, C. J. Liu, Z. Y. Zeng, H. Zhang, C. M. Zhou, X. L. Jia and Y. H. Yang, *J. Catal.*, 2012, **289**, 105-117.
- 23 F. Li, Q. H. Zhang and Y. Wang, *Appl. Catal. A-Gen.*, 2008, **334**, 217-226.

- 24 H. L. Liu, Y. L. Liu, Y. W. Li, Z. Y. Tang and H. F. Jiang, *J. Phys. Chem. C*, 2010, **114**, 13362-13369.
- 25 Y. Hao, G. P. Hao, D. C. Guo, C. Z. Guo, W. C. Li, M. R. Li and A. H. Lu, *ChemCatChem*, 2012, **4**, 1595-1602.
- 26 G. J. Wu, X. M. Wang, N. I. J. Guan and L. D. Li, *Appl. Catal. B-Environ*, 2013, **136**, 177-185.
- 27 P. F. Zhang, Y. T. Gong, H. R. Li, Z. R. Chen and Y. Wang, *Nat. Commun.*, 2013, **4**, 1593.
- 28 J. V. Liebig, *Ann. Pharm.*, 1834, **10**, 10.
- 29 E. C. Franklin, *J. Am. Chem. Soc.*, 1922, **44**, 486-509.
- 30 M. L. Cohen, *Phys. Rev. B*, 1985, **32**, 7988-7991.
- 31 A. Y. Liu and M. L. Cohen, *Science*, 1989, **245**, 841-842.
- 32 M. L. Cohen, *Science*, 1993, **261**, 307-308.
- 33 D. M. Teter and R. J. Hemley, *Science*, 1996, **271**, 53-55.
- 34 J. L. Corkill and M. L. Cohen, *Phys. Rev. B*, 1993, **48**, 17622-17624.
- 35 A. Y. Liu and R. M. Wentzcovitch, *Phys. Rev. B*, 1994, **50**, 10362-10365.
- 36 J. E. Lowther, *Phys. Rev. B*, 1999, **59**, 11683-11686.
- 37 J. Ortega and O. F. Sankey, *Phys. Rev. B*, 1995, **51**, 2624-2627.
- 38 E. Kroke and M. Schwarz, *Coordin. Chem. Rev.*, 2004, **248**, 493-532.
- 39 Y. Miyamoto, M. L. Cohen and S. G. Louie, *Solid State Commun.*, 1997, **102**, 605-608.
- 40 J. Kouvetakis, M. Todd, B. Wilkens, A. Bandari and N. Cave, *Chem. Mater.*, 1994, **6**, 811-814.
- 41 C. Li, C.-B. Cao and H.-S. Zhu, *Mater. Lett.*, 2004, **58**, 1903-1906.
- 42 B. V. Lotsch and W. Schnick, *Chem. Mater.*, 2006, **18**, 1891-1900.
- 43 Y.-G. Yoon, B. G. Pfrommer, F. Mauri and S. G. Louie, *Phys. Rev. Lett.*, 1998, **80**, 3388-3391.
- 44 I. Alves, G. Demazeau, B. Tanguy and F. Weill, *Solid State Commun.*, 1999, **109**, 697-701.
- 45 Z. Zhang, K. Leinenweber, M. Bauer, L. A. J. Garvie, P. F. McMillan and G. H. Wolf, *J. Am. Chem. Soc.*, 2001, **123**, 7788-7796.
- 46 M. Mattesini, S. F. Matar, A. Snis, J. Etourneau and A. Mavromaras, *J. Mater. Chem.*, 1999, **9**, 3151-3158.
- 47 A. Snis and S. F. Matar, *Phys. Rev. B*, 1999, **60**, 10855-10863.
- 48 H. Montigaud, B. Tanguy, G. Demazeau, I. Alves, M. Birot and J. Dunogues, *Diam. Relat. Mater.*, 1999, **8**, 1707-1710.
- 49 V. N. Khabashesku, J. L. Zimmerman and J. L. Margrave, *Chem. Mater.*, 2000, **12**, 3264-3270.

- 50 J. L. Zimmerman, R. Williams, V. N. Khabashesku and J. L. Margrave, *Nano Lett.*, 2001, **1**, 731-734.
- 51 E. Kroke, M. Schwarz, E. Horath-Bordon, P. Kroll, B. Noll and A. D. Norman, *New J. Chem.*, 2002, **26**, 508-512.
- 52 G. M. Rignanese, J. C. Charlier and X. Gonze, *Phys. Rev. B*, 2002, **66**, 205416.
- 53 Y. Zhang, H. Sun and C. Chen, *Phys. Rev. B*, 2006, **73**, 144115.
- 54 Y. Wang, X. Wang and M. Antonietti, *Angew. Chem. Int. Ed.*, 2012, **51**, 68-89.
- 55 L. Gmelin, *Ann. Pharm.*, 1835, **15**, 252.
- 56 J. V. Liebig, *Ann. Chem. Pharm.*, 1850, **50**, 337.
- 57 J. V. Liebig, *Ann. Chem. Pharm.*, 1850, **73**, 257.
- 58 H. J. May, *Appl. Chem.*, 1959, 240.
- 59 J. Sehnert, K. Baerwinkel and J. Senker, *J. Phys. Chem. B*, 2007, **111**, 10671-10680.
- 60 E. Horvath-Bordon, E. Kroke, I. Svoboda, H. Fuess and R. Riedel, *New J. Chem.*, 2005, **29**, 693-699.
- 61 T. Komatsu and T. Nakamura, *J. Mater. Chem.*, 2001, **11**, 474-478.
- 62 M. J. Bojdys, J.-O. Müller, M. Antonietti and A. Thomas, *Chem.-Eur. J.*, 2008, **14**, 8177-8182.
- 63 A. Sattler, S. Pagano, M. Zeuner, A. Zurawski, D. Gunzelmann, J. Senker, K. Müller-Buschbaum and W. Schnick, *Chem.-Eur. J.*, 2009, **15**, 13161-13170.
- 64 B. V. Lotsch and W. Schnick, *Chem.-Eur. J.*, 2007, **13**, 4956-4968.
- 65 T. Komatsu, *J. Mater. Chem.*, 2001, **11**, 799-801.
- 66 T. Komatsu, *J. Mater. Chem.*, 2001, **11**, 802-803.
- 67 D. S. Su, J. Zhang, B. Frank, A. Thomas, X. C. Wang, J. Paraknowitsch and R. Schlogl, *ChemSusChem*, 2010, **3**, 169-180.
- 68 X. Wang, K. Maeda, A. Thomas, K. Takanae, G. Xin, J. M. Carlsson, K. Domen and M. Antonietti, *Nat. Mater.*, 2009, **8**, 76-80.
- 69 X. Jin, V. V. Balasubramanian, S. T. Selvan, D. P. Sawant, M. A. Chari, G. Q. Lu and A. Vinu, *Angew. Chem. Int. Ed.*, 2009, **48**, 7884-7887.
- 70 Y. Wang, J. Yao, H. R. Li, D. S. Su and M. Antonietti, *J. Am. Chem. Soc.*, 2011, **133**, 2362-2365.
- 71 X.-H. Li and M. Antonietti, *Chem. Soc. Rev.*, 2013, **42**, 6593-6604.
- 72 F. Goettmann, A. Fischer, M. Antonietti and A. Thomas, *Angew. Chem. Int. Ed.*, 2006, **45**, 4467-4471.
- 73 F. Goettmann, A. Fischer, M. Antonietti and A. Thomas, *Chem. Commun.*, 2006, 4530-4532.
- 74 D. E. De Vos, M. Dams, B. F. Sels and P. A. Jacobs, *Chem. Rev.*, 2002, **102**, 3615-3640.
- 75 I. Hermans, P. A. Jacobs and J. Peeters, *Chem.-Eur. J.*, 2006, **12**, 4229-4240.

- 76 F. Li, M. Wang, C. B. Ma, A. P. Gao, H. B. Chen and L. C. Sun, *Dalton. Trans.*, 2006, 2427-2434.
- 77 C. He, J. J. Li, P. Li, J. Cheng, Z. P. Hao and Z. P. Xu, *Appl. Catal. B-Environ*, 2010, **96**, 466-475.
- 78 H. Z. Liu, T. Jiang, B. X. Han, S. G. Liang and Y. X. Zhou, *Science*, 2009, **326**, 1250-1252.
- 79 N. Herron and C. A. Tolman, *J. Am. Chem. Soc.*, 1987, **109**, 2837-2839.
- 80 R. Bal, M. Tada, T. Sasaki and Y. Iwasawa, *Angew. Chem. Int. Ed.*, 2006, **45**, 448-452.
- 81 X. Chen, J. Zhang, X. Fu, M. Antonietti and X. Wang, *J. Am. Chem. Soc.*, 2009, **131**, 11658-11659.
- 82 Y. Wang, X. C. Wang, M. Antonietti and Y. J. Zhang, *ChemSusChem*, 2010, **3**, 435-439.
- 83 A. B. D.Ferri, *Top. Catal.*, 2009, **52**, 1323-1333.
- 84 S. A. Tromp, I. Matijošytė, R. A. Sheldon, I. W. C. E. Arends, G. Mul, M. T. Kreutzer, J. A. Moulijn and S. de Vries, *ChemCatChem*, 2010, **2**, 827-833.
- 85 R. A. Sheldon, I. Arends, G. J. Ten Brink and A. Dijkman, *Accounts. Chem. Res.*, 2002, **35**, 774-781.
- 86 F. Su, S. C. Mathew, G. Lipner, X. Fu, M. Antonietti, S. Blechert and X. Wang, *J. Am. Chem. Soc.*, 2010, **132**, 16299-16301.
- 87 L. Zhang, D. Liu, J. Guan, X. Chen, X. Guo, F. Zhao, T. Hou and X. Mu, *Mater. Res. Bull.*, 2014, **59**, 84-92.
- 88 B. Long, Z. Ding and X. Wang, *ChemSusChem*, 2013, **6**, 2074-2078.
- 89 Y. Chen, J. S. Zhang, M. W. Zhang and X. C. Wang, *Chem. Sci.*, 2013, **4**, 3244-3248.
- 90 Z. S. Zheng and X. S. Zhou, *Chin. J. Chem.*, 2012, **30**, 1683-1686.
- 91 J. Gawronski, N. Wascinska and J. Gajewy, *Chem. Rev.*, 2008, **108**, 5227-5252.
- 92 K. C. Nicolaou, C. J. N. Mathison and T. Montagnon, *Angew. Chem. Int. Ed.*, 2003, **42**, 4077-4082.
- 93 F. Su, S. C. Mathew, L. Mühlmann, M. Antonietti, X. Wang and S. Blechert, *Angew. Chem. Int. Ed.*, 2011, **50**, 657-660.
- 94 L. Mühlmann, M. Baar, J. Riess, M. Antonietti, X. C. Wang and S. Blechert, *Adv. Synth. Catal.*, 2012, **354**, 1909-1913.
- 95 T. Song, B. Zhou, G. W. Peng, Q. B. Zhang, L. Z. Wu, Q. Liu and Y. Wang, *Chem.-Eur. J.*, 2014, **20**, 678-682.
- 96 M. Sako, H. Hosokawa, T. Ito and M. Iinuma, *J. Org. Chem.*, 2004, **69**, 2598-2600.
- 97 S. Nicotra, M. R. Cramarossa, A. Mucci, U. M. Pagnoni, S. Riva and L. Forti, *Tetrahedron*, 2004, **60**, 595-600.
- 98 P. Waffo-Teguo, D. Lee, M. Cuendet, J.-M. Méillon, J. M. Pezzuto and A. D. Kinghorn, *J. Nat. Prod.*, 2000, **64**, 136-138.

- 99 Y. Di, X. C. Wang, A. Thomas and M. Antonietti, *ChemCatChem*, 2010, **2**, 834-838.
- 100 P. F. Zhang, Y. T. Gong, H. R. Li, Z. R. Chen and Y. Wang, *Rsc Adv.*, 2013, **3**, 5121-5126.
- 101 X. Ye, Y. Cui, X. Qiu and X. Wang, *Appl. Catal. B- Environ.*, 2014, **152-153**, 383-389.
- 102 X. Ye, Y. Cui and X. Wang, *ChemSusChem*, 2014, **7**, 738-742.
- 103 X. Ye, Y. Zheng and X. Wang, *Chin. J. Chem.*, 2014, **32**, 498-506.
- 104 P. Zhang, H. Li and Y. Wang, *Chem. Commun.*, 2014, **50**, 6312-6315.
- 105 P. F. Zhang, Y. Wang, H. R. Li and M. Antonietti, *Green Chem.*, 2012, **14**, 1904-1908.
- 106 P. F. Zhang, Y. Wang, J. Yao, C. M. Wang, C. Yan, M. Antonietti and H. R. Li, *Adv. Synth. Catal.*, 2011, **353**, 1447-1451.
- 107 K. Chen, Y. Sun, C. Wang, J. Yao, Z. Chen and H. Li, *Phys. Chem. Chem. Phys.*, 2012, **14**, 12141-12146.
- 108 J. Liu, Y. Yang, N. Liu, Y. Liu, H. Huang and Z. Kang, *Green Chem.*, 2014, 4559-4565.
- 109 G. Cantarella, C. Galli and P. Gentili, *J. Mol. Catal. B-Enzym.*, 2003, **22**, 135-144.
- 110 Y. Ishii, T. Iwahama, S. Sakaguchi, K. Nakayama and Y. Nishiyama, *J. Org. Chem.*, 1996, **61**, 4520-4526.
- 111 S. Coseri, *Catal. Rev.*, 2009, **51**, 218-292.
- 112 S. C. Yan, Z. S. Li and Z. G. Zou, *Langmuir*, 2009, **25**, 10397-10401.
- 113 S. C. Yan, Z. S. Li and Z. G. Zou, *Langmuir*, 2010, **26**, 3894-3901.
- 114 S. C. Yan, S. B. Lv, Z. S. Li and Z. G. Zou, *Dalton. Trans.*, 2010, **39**, 1488-1491.
- 115 E. C. McLaughlin, H. Choi, K. Wang, G. Chiou and M. P. Doyle, *J. Org. Chem.*, 2009, **74**, 730-738.
- 116 J. A. R. Salvador and J. H. Clark, *Green Chem.*, 2002, **4**, 352-356.
- 117 Z. Yao, X. B. Hu, J. Y. Mao and H. R. Li, *Green Chem.*, 2009, **11**, 2013-2017.
- 118 M. A. Foustieris, A. I. Koutsourea, S. S. Nikolaropoulos, A. Riahi and J. Muzart, *J. Mol. Catal. A-Chem.*, 2006, **250**, 70-74.
- 119 G. Y. Liu, R. R. Tang and Z. Wang, *Catal. Lett.*, 2014, **144**, 717-722.
- 120 C. Einhorn, J. Einhorn, C. Marcadal and J. L. Pierre, *Chem. Commun.*, 1997, 726-726.
- 121 T. V. Rao, B. Sain, K. Kumar, P. S. Murthy, T. Rao and G. C. Joshi, *Synthetic. Commun.*, 1998, **28**, 319-326.
- 122 A. D. Malievskii, *Petrol. Chem.*, 2008, **48**, 40-45.
- 123 Y. Wang, H. R. Li, J. Yao, X. C. Wang and M. Antonietti, *Chem. Sci.*, 2011, **2**, 446-450.
- 124 M. B. Ansari, B. H. Min, Y. H. Mo and S. E. Park, *Green Chem.*, 2011, **13**, 1416-1421.
- 125 X. H. Li, X. C. Wang and M. Antonietti, *ACS Catal.*, 2012, **2**, 2082-2086.
- 126 X. H. Li, J. S. Chen, X. C. Wang, J. H. Sun and M. Antonietti, *J. Am. Chem. Soc.*, 2011, **133**, 8074-8077.
- 127 A. E. Shilov and G. B. Shul'pin, *Chem. Rev.*, 1997, **97**, 2879-2932.

- 128 C. Jia, T. Kitamura and Y. Fujiwara, *Accounts. Chem. Res.*, 2001, **34**, 633-639.
- 129 L. Kesavan, R. Tiruvalam, M. H. Ab Rahim, M. I. bin Saiman, D. I. Enache, R. L. Jenkins, N. Dimitratos, J. A. Lopez-Sanchez, S. H. Taylor, D. W. Knight, C. J. Kiely and G. J. Hutchings, *Science*, 2011, **331**, 195-199.
- 130 W. Nam, *Accounts. Chem. Res.*, 2007, **40**, 465-465.
- 131 F. Konietzki, U. Kolb, U. Dingerdissen and W. F. Maier, *J. Catal.*, 1998, **176**, 527-535.
- 132 F. Wang, J. Xu, X. Li, J. Gao, L. Zhou and R. Ohnishi, *Adv. Synth. Catal.*, 2005, **347**, 1987-1992.
- 133 B. H. Min, M. B. Ansari, Y. H. Mo and S. E. Park, *Catal. Today*, 2013, **204**, 156-163.
- 134 K. M. Jinka, J. Sebastian and R. V. Jasra, *J. Mol. Catal. A-Chem.*, 2007, **274**, 33-41.
- 135 M. B. Ansari, H. Jin and S.-E. Park, *Catal. Sci. Technol.*, 2013, **3**, 1261.
- 136 R. Kumar, S. Sithambaram and S. L. Suib, *J. Catal.*, 2009, **262**, 304-313.
- 137 L. Liu, Y. Li, H. Wei, M. Dong, J. Wang, A. M. Z. Slawin, J. Li, J. Dong and R. E. Morris, *Angew. Chem. Int. Ed.*, 2009, **48**, 2206-2209.
- 138 M. J. L. Kishore and A. Kumar, *Aiche J.*, 2007, **53**, 1550-1561.
- 139 Y. Wang, J. Zhang, X. Wang, M. Antonietti and H. Li, *Angew. Chem. Int. Ed.*, 2010, **49**, 3356-3359.
- 140 Z. Ding, X. Chen, M. Antonietti and X. Wang, *ChemSusChem*, 2011, **4**, 274-281.
- 141 G. Ding, W. Wang, T. Jiang, B. Han, H. Fan and G. Yang, *ChemCatChem*, 2013, **5**, 192-200.
- 142 Z. Long, Y. Zhou, G. Chen, W. Ge and J. Wang, *Sci. Rep.*, 2014, **4**, 3651.
- 143 C. E. Chan-Thaw, A. Villa, G. M. Veith, K. Kailasam, L. A. Adamczyk, R. R. Unocic, L. Prati and A. Thomas, *Chem.-Asian. J.*, 2012, **7**, 387-393.
- 144 Y. Zhang-Steenwinkel, L. M. van der Zande, H. L. Casticum and A. Bliet, *Appl. Catal. B- Environ.*, 2004, **54**, 93-103.
- 145 J. Zhu, S. A. C. Carabineiro, D. Shan, J. L. Faria, Y. Zhu and J. L. Figueiredo, *J. Catal.*, 2010, **274**, 207-214.
- 146 J. A. Singh, S. H. Overbury, N. J. Dudley, M. Li and G. M. Veith, *ACS Catal.*, 2012, **2**, 1138-1146.
- 147 P. Xiao, Y. Zhao, T. Wang, Y. Zhan, H. Wang, J. Li, A. Thomas and J. Zhu, *Chem.-Eur. J.*, 2014, **20**, 2872-2878.
- 148 J. Guzman and B. C. Gates, *J. Am. Chem. Soc.*, 2004, **126**, 2672-2673.
- 149 A. C. Gluhoi, H. S. Vreeburg, J. W. Bakker and B. E. Nieuwenhuys, *Appl. Catal. A-Gen.*, 2005, **291**, 145-150.
- 150 Y. Li, Y. T. Gong, X. Xu, P. F. Zhang, H. R. Li and Y. Wang, *Catal. Commun.*, 2012, **28**, 9-12.

- 151 Y. T. Gong, P. F. Zhang, X. Xu, Y. Li, H. R. Li and Y. Wang, *J. Catal.*, 2013, **297**, 272-280.
- 152 Y. Li, X. Xu, P. F. Zhang, Y. T. Gong, H. R. Li and Y. Wang, *Rsc Adv.*, 2013, **3**, 10973-10982.
- 153 D. S. Deng, Y. Yang, Y. T. Gong, Y. Li, X. Xu and Y. Wang, *Green Chem.*, 2013, **15**, 2525-2531.
- 154 M. Chatterjee, H. Kawanami, M. Sato, A. Chatterjee, T. Yokoyama and T. Suzuki, *Adv. Synth. Catal.*, 2009, **351**, 1912-1924.
- 155 B. Chen, U. Dingerdissen, J. G. E. Krauter, H. Rotgerink, K. Mobus, D. J. Ostgard, P. Panster, T. H. Riermeier, S. Seebald, T. Tacke and H. Trauthwein, *Appl. Catal. A-Gen.*, 2005, **280**, 17-46.
- 156 S. Watanabe and V. Arunajatesan, *Top. Catal.*, 2010, **53**, 1150-1152.
- 157 C. Zhao, S. Kasakov, J. Y. He and J. A. Lercher, *J. Catal.*, 2012, **296**, 12-23.
- 158 R. T. Shuman, P. L. Ornstein, J. W. Paschal and P. D. Gesellchen, *J. Org. Chem.*, 1990, **55**, 738-741.
- 159 A. R. Katritzky, S. Rachwal and B. Rachwal, *Tetrahedron*, 1996, **52**, 15031-15070.
- 160 S. Gomez, J. A. Peters and T. Maschmeyer, *Adv. Synth. Catal.*, 2002, **344**, 1037-1057.
- 161 R. Reguillo, M. Grellier, N. Vautravers, L. Vendier and S. Sabo-Etienne, *J. Am. Chem. Soc.*, 2010, **132**, 7854-+.
- 162 S. Enthaler, D. Addis, K. Junge, G. Erre and M. Beller, *Chem.-Eur. J.*, 2008, **14**, 9491-9494.
- 163 S. Enthaler, K. Junge, D. Addis, G. Erre and M. Beller, *ChemSusChem*, 2008, **1**, 1006-1010.
- 164 R. A. Grey, G. P. Pez and A. Wallo, *J. Am. Chem. Soc.*, 1981, **103**, 7536-7542.
- 165 J. R. L. Burwell, *Chem. Rev.*, 1957, **57**, 895-934.
- 166 E. N. Marvell and T. Li, *Synthesis-stuttgart*, 1973, 457-468.
- 167 S. W. Bian, Z. Ma and W. G. Song, *J. Phys. Chem. C*, 2009, **113**, 8668-8672.
- 168 X. H. Li, X. C. Wang and M. Antonietti, *Chem. Sci.*, 2012, **3**, 2170-2174.
- 169 K. Maeda, X. C. Wang, Y. Nishihara, D. L. Lu, M. Antonietti and K. Domen, *J. Phys. Chem. C*, 2009, **113**, 4940-4947.
- 170 T. Fu, M. Wang, W. Cai, Y. Cui, F. Gao, L. Peng, W. Chen and W. Ding, *ACS Catal.*, 2014, **4**, 2536-2543.
- 171 L.-H. Gong, Y.-Y. Cai, X.-H. Li, Y.-N. Zhang, J. Su and J.-S. Chen, *Green Chem.*, 2014, **16**, 3746.
- 172 J. H. Lee, J. Ryu, J. Y. Kim, S.-W. Nam, J. H. Han, T.-H. Lim, S. Gautam, K. H. Chae and C. W. Yoon, *J. Mater. Chem. A*, 2014, **2**, 9490.

- 173 Z.-L. Wang, J.-M. Yan, Y. Ping, H.-L. Wang, W.-T. Zheng and Q. Jiang, *Angew. Chem. Int. Ed.*, 2013, **52**, 4406-4409.
- 174 S. Zhang, Ö. Metin, D. Su and S. Sun, *Angew. Chem. Int. Ed.*, 2013, **52**, 3681-3684.
- 175 U. Vongunten and J. Holgne, *Environ. Sci. Technol.*, 1994, **28**, 1234-1242.
- 176 H. S. Weinberg, C. A. Delcomyn and V. Unnam, *Environ. Sci. Technol.*, 2003, **37**, 3104-3110.
- 177 H. Chen, Z. Y. Xu, H. Q. Wan, J. Z. Zheng, D. Q. Yin and S. R. Zheng, *Appl. Catal. B-Environ*, 2010, **96**, 307-313.
- 178 P. Zhang, F. Jiang and H. Chen, *Chem. Eng. J.*, 2013, **234**, 195-202.
- 179 Y.-Y. Cai, X.-H. Li, Y.-N. Zhang, X. Wei, K.-X. Wang and J.-S. Chen, *Angew. Chem. Int. Ed.*, 2013, **52**, 11822-11825.
- 180 Y.-S. Jun, E. Z. Lee, X. Wang, W. H. Hong, G. D. Stucky and A. Thomas, *Adv. Funct. Mater.*, 2013, **23**, 3661-3667.
- 181 M. Li, X. Xu, Y. Gong, Z. Wei, Z. Hou, H. Li and Y. Wang, *Green Chem.*, 2014, **16**, 4371-4377.
- 182 X. Xu, M. Tang, M. Li, H. Li and Y. Wang, *ACS Catal.*, 2014, **4**, 3132-3135.
- 183 H. Jin, T. Xiong, Y. Li, X. Xu, M. Li and Y. Wang, *Chem. Commun.*, 2014, **50**, 12637-12640.